

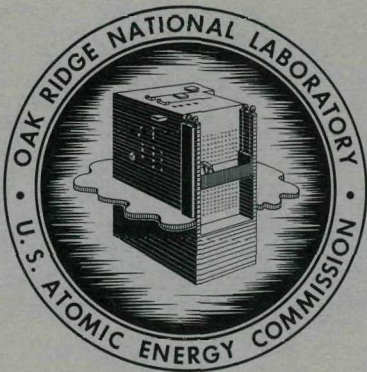
MASTER

3 25-
8-14-61
AUG 16 1961

ORNL-3086
UC-38 - Engineering and Equipment
TID-4500 (16th ed.)

CALCULATED TRANSIENT PRESSURES DUE TO
IMPULSE AND RAMP PERTURBATIONS TO
VENTILATING SYSTEMS IN
BUILDINGS 3019, 3026, 3508, AND 4507

J. J. Perona
W. E. Dunn
H. F. Johnson



OAK RIDGE NATIONAL LABORATORY

operated by

UNION CARBIDE CORPORATION

for the

U.S. ATOMIC ENERGY COMMISSION

DISCLAIMER

This report was prepared as an account of work sponsored by an agency of the United States Government. Neither the United States Government nor any agency Thereof, nor any of their employees, makes any warranty, express or implied, or assumes any legal liability or responsibility for the accuracy, completeness, or usefulness of any information, apparatus, product, or process disclosed, or represents that its use would not infringe privately owned rights. Reference herein to any specific commercial product, process, or service by trade name, trademark, manufacturer, or otherwise does not necessarily constitute or imply its endorsement, recommendation, or favoring by the United States Government or any agency thereof. The views and opinions of authors expressed herein do not necessarily state or reflect those of the United States Government or any agency thereof.

DISCLAIMER

Portions of this document may be illegible in electronic image products. Images are produced from the best available original document.

Printed in USA. Price \$1.50. Available from the
Office of Technical Services
Department of Commerce
Washington 25, D. C.

LEGAL NOTICE

This report was prepared as an account of Government sponsored work. Neither the United States, nor the Commission, nor any person acting on behalf of the Commission:

- A. Makes any warranty or representation, expressed or implied, with respect to the accuracy, completeness, or usefulness of the information contained in this report, or that the use of any information, apparatus, method, or process disclosed in this report may not infringe privately owned rights; or
- B. Assumes any liabilities with respect to the use of, or for damages resulting from the use of any information, apparatus, method, or process disclosed in this report.

As used in the above, "person acting on behalf of the Commission" includes any employee or contractor of the Commission, or employee of such contractor, to the extent that such employee or contractor of the Commission, or employee of such contractor prepares, disseminates, or provides access to, any information pursuant to his employment or contract with the Commission, or his employment with such contractor.

ORNL-3086

Contract No. W-7405-eng-26

CHEMICAL TECHNOLOGY DIVISION

Unit Operations Section

CALCULATED TRANSIENT PRESSURES DUE TO IMPULSE AND
RAMP PERTURBATIONS TO VENTILATING SYSTEMS IN
BUILDINGS 3019, 3026, 3508, AND 4507

J. J. Perona
W. E. Dunn
H. F. Johnson

DATE ISSUED

AUG 15 1951

OAK RIDGE NATIONAL LABORATORY
Oak Ridge, Tennessee
Operated by
UNION CARBIDE CORPORATION
for the
U. S. Atomic Energy Commission

ABSTRACT

As part of a general hazard review survey conducted by the Chemical Technology Division of its facilities, transient pressures due to impulse and ramp perturbations to the cell ventilating systems of buildings 3019, 3026, and 4607 and the closed glove box system of 3508 were calculated. From the portions of the pressure curves above atmospheric pressure, volumes of gas outleakage were estimated; thus the amount of activity released can be calculated if an estimate of the activity concentration is available.

The volumes of outleakage for all four ventilating systems were small for reasonable sizes of perturbations. For an impulse perturbation causing an instantaneous rise of + 8.0 in. H₂O, the length of time above atmospheric pressure and estimated outleakages for PRFP cells in 3019 are 1.5 sec and 3.1 ft³, respectively; for volatility cell 1 in 3019, 0.33 sec and 0.45 ft³; for cell A in 3026, 2.1 sec and 3.0 ft³; for a glove box in 3508, 0.066 sec and 0.04 ft³; and a cell in 4507, 0.26 sec and 0.03 ft³.

CONTENTS

	<u>Page</u>
1.0 Introduction	4
2.0 General Approach	4
2.1 Derivation of Equations	4
2.2 Introduction of Perturbations	6
2.3 Calculation of Outleakage	6
3.0 Cell Ventilation System in Bldg. 3019	7
3.1 Description of Ventilating System	7
3.2 Assumptions and Equations	7
3.3 Analog Solution	11
3.4 Results	11
4.0 Cell Ventilation System in Bldg. 3026	20
4.1 Description of Ventilating System	20
4.2 Mathematical Treatment and Analog Circuit Development	23
4.3 Results	36
5.0 Closed Glove-box System in Bldg. 3508	44
5.1 Description of Ventilating System	44
5.2 Assumptions and Equations	46
5.3 Analog Computer Circuitry	48
5.4 Results	48
6.0 Cell Ventilation System in Bldg. 4507	53
6.1 Description of Ventilation System	53
6.2 Mathematical Model	58
6.3 Transient Response to Step Change in Cell Pressure	59
6.4 Transient Response to Ramp Perturbations	60

1.0 INTRODUCTION

As an adjunct to the redesign of the ventilating systems of several cells and buildings in which experimentation and processing of radioactive materials are carried out by the Chemical Technology Division, the transient behavior of the newly designed ventilating systems was analyzed. Pressures were calculated throughout each ventilating system as a function of time as each system recovered from impulse perturbations, as might be caused by an explosion, and from ramp perturbations, as might be caused by the rupture of a gas line. Thus, the length of time that the pressure in a cell or glove box would be above atmospheric pressure was obtained and the total amount of outleakage estimated.

The cell ventilating systems in Bldg. 3019, 3026, and 4507, and the glove box ventilating system in Bldg. 3508 were studied. The results of the calculations presented in this report should be helpful in evaluating the degree of hazard associated with the operations carried out in these buildings. A formal hazard evaluation including the above-mentioned buildings is being prepared (ORNL-2956).

The ventilating systems which were studied had not yet been installed at the time these calculations were made but were in the final design stage. Therefore the details of the ventilating systems as described in this report may not be entirely accurate, and the report should not be used as a reference for details of the installed systems.

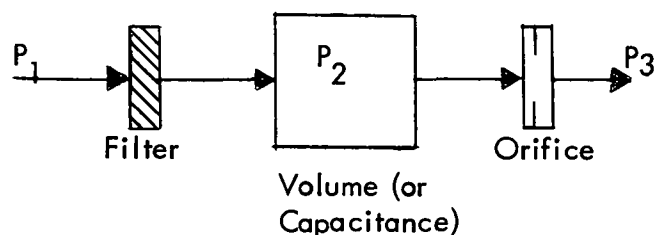
The authors are indebted for information on the proposed ventilating systems to E. J. Frederick, V. J. Kelleghan, A. M. Rom, W. J. Stockdale, and W. R. Winsbro.

2.0 GENERAL APPROACH

A set of differential equations was derived for each ventilating system, relating pressures, volumes, and resistances to flow. Nearly all these equations were nonlinear, so that solution on an analog computer was expedient. Only one differential equation was required to represent the operation of the ventilating system in Bldg. 4507, and graphical solutions for this system were carried out by hand.

2.1 Derivation of Equations

The method of derivation of the differential equations may be illustrated with reference to a schematic segment of a ventilating system:



The resistance to flow of the filter is given by Darcy's equation, which may be simplified for fixed filter thickness and fixed fluid viscosity to

$$Q = (P_1 - P_2)/R_F \quad (2-1)$$

where Q = flow rate

$P_1 - P_2$ = pressure drop across filter

R_F = resistance of filter

The resistance to flow of the orifice is given by

$$Q = (P_2 - P_3)^{1/2}/R_O \quad (2-2)$$

where $P_2 - P_3$ = pressure drop across orifice

R_O = resistance of orifice

In the case of unsteady flows, input - output = accumulation and

$$\frac{P_1 - P_2}{R_F} - \frac{(P_2 - P_3)^{1/2}}{R_O} = \frac{dN}{dt} = \frac{V}{RT} \frac{dP_2}{dt} \quad (2-3)$$

where N = number of moles of air in the capacitance

t = time

V = volume of capacitance

R = gas constant

T = temperature

No pressure drop was assumed to occur in the duct work, and the ideal gas law was assumed. Note that the steady-state pressure relation is obtained on setting dN/dt equal to zero. Proceeding in the same way, equations were written for each capacitance in a ventilating system. Valves were treated as orifices. Values for the resistance constants were obtained from steady-state data. Resistance constants for filters were calculated assuming that the filters were clean. The treatment of special items such as blowers and automatic controllers is discussed in the following sections as the need arises.

When pressure drop can change sign across an orifice or valve, the application of eq. 2-2 can result in some difficulty because the sign change occurs within the square root radical and results in an imaginary number rather than changing the sign on Q . In these cases, where flow can occur in either direction, eq. 2-2 should be replaced by

$$Q = \frac{P_2 - P_3}{R_0} \left(|P_2 - P_3| \right)^{-1/2} \quad (2-2')$$

The square root circuitry using a servomultiplier, as, for example, in Fig. 3, achieves the results of eq. 2-2'.

2.2 Introduction of Perturbations

Impulse perturbations were introduced by instantaneously changing the pressure in the capacitance in question. Where the analog computer was used, this was done by changing the initial condition setting on the integrating amplifier in question to a value higher than the steady-state value before switching the computer to the "operate" position.

The introduction of a constant-rate air source to the capacitance in question was termed a "ramp perturbation." This was done by adding a constant to the differential equation describing the behavior of a capacitance. For example, the behavior of the system sketched in Sect. 2.1 during a ramp perturbation would be described by

$$\frac{dP_2}{dt} = \frac{RT}{R_F V} (P_1 - P_2) + K - \frac{RT}{R_0 V} (P_2 - P_3)^{1/2} \quad (2-3')$$

in which K has the units in. H₂O/sec.

2.3 Calculation of Outleakage

The total amount of gases leaked out of a cell during the period when it is above atmospheric pressure may be calculated from

$$L = \frac{1}{R_L} \int_0^t (P)^{1/2} dt \quad (2-4)$$

where L = outleakage, ft³

R_L = resistance, (in. H₂O)^{1/2}/(ft³/sec)

P = pressure relative to atmospheric, in. H₂O

and zero to t is the time in seconds during which P is larger than zero. R_L can be calculated from eq 2-2 if the inleakage rate is known during steady-state operation. According to the formal hazard evaluation (ORNL-2956), the leakage rate under normal operating conditions should not exceed 1% of the cell volume per minute.

3.0 CELL VENTILATION SYSTEM IN BLDG. 3019

3.1 Description of Ventilating System

Of the seven cells in Bldg. 3019, two (cells 1 and 2) are used for the Fluoride Volatility process and five (cells 3 through 7) are designated the "power reactor fuel processing" cells. All seven cells are connected to a common off-gas header, 4 ft by 4.5 ft in cross section, which runs the length of the building (166 ft). A 36-in.-dia duct 146 ft in length connects the off-gas header to a filter house containing 21 Airmat deep-bed-pocket type A filters in parallel, which are connected in series with 18 absolute filters in parallel. From the filter house the off-gases pass through a blower to the 3020 stack.

The high-level Volatility processing equipment is in cell 1, with a portion of cell 1 (called cell 1A) and cell 2 acting as secondary containment areas (Fig. 1). Atmospheric air passes through a roughing filter and a manually set valve into cell 1. Atmospheric air also passes through a roughing filter into cells 1A and 2 and then through a check valve and orifice assembly. The air from the Volatility cells is scrubbed in a spray chamber for HF removal before passing into the building off-gas header. Cell volumes and steady-state flow rates are given in Fig. 1.

The five PRFP cells are identical except for cell 7, which is twice the size of the other cells and has two inlet and two outlet ducts instead of one each. In Fig. 1 one PRFP cell is shown as having its roof removed, one as in normal operation, and the others as a single, large, equivalent cell. Perturbations were applied to the single, normally connected cell. Atmospheric air passes through a manually set valve, a roughing filter and a check valve into each PRFP cell, and out through a check valve and orifice assembly into the building off-gas header. The check valves at the cell inlets are to prevent backflow out of a cell in the event that the cell pressure should rise above atmospheric. The check valves at the cell outlets are to prevent the flow of air from one cell into another through the header in the event of an incident in a cell. The orifices in the cell outlets permit effective operation of the ventilating system in the event that the roof is removed from a cell. An additional stream enters the off-gas header from a pipe tunnel through a manually set valve.

3.2 Assumptions and Equations

The resistances of the valves, orifices, and filters are given in Table 1. The steady-state pressures through the system, as determined from the steady-state flow equations, are:

$P_1 = - 1.50 \text{ in. H}_2\text{O}$	$P_4 = - 2.62 \text{ in. H}_2\text{O}$
$P_2 = - 1.57$	$P_5 = - 15.8$
$P_3 = - 1.86$	$P_6 = - 1.50$

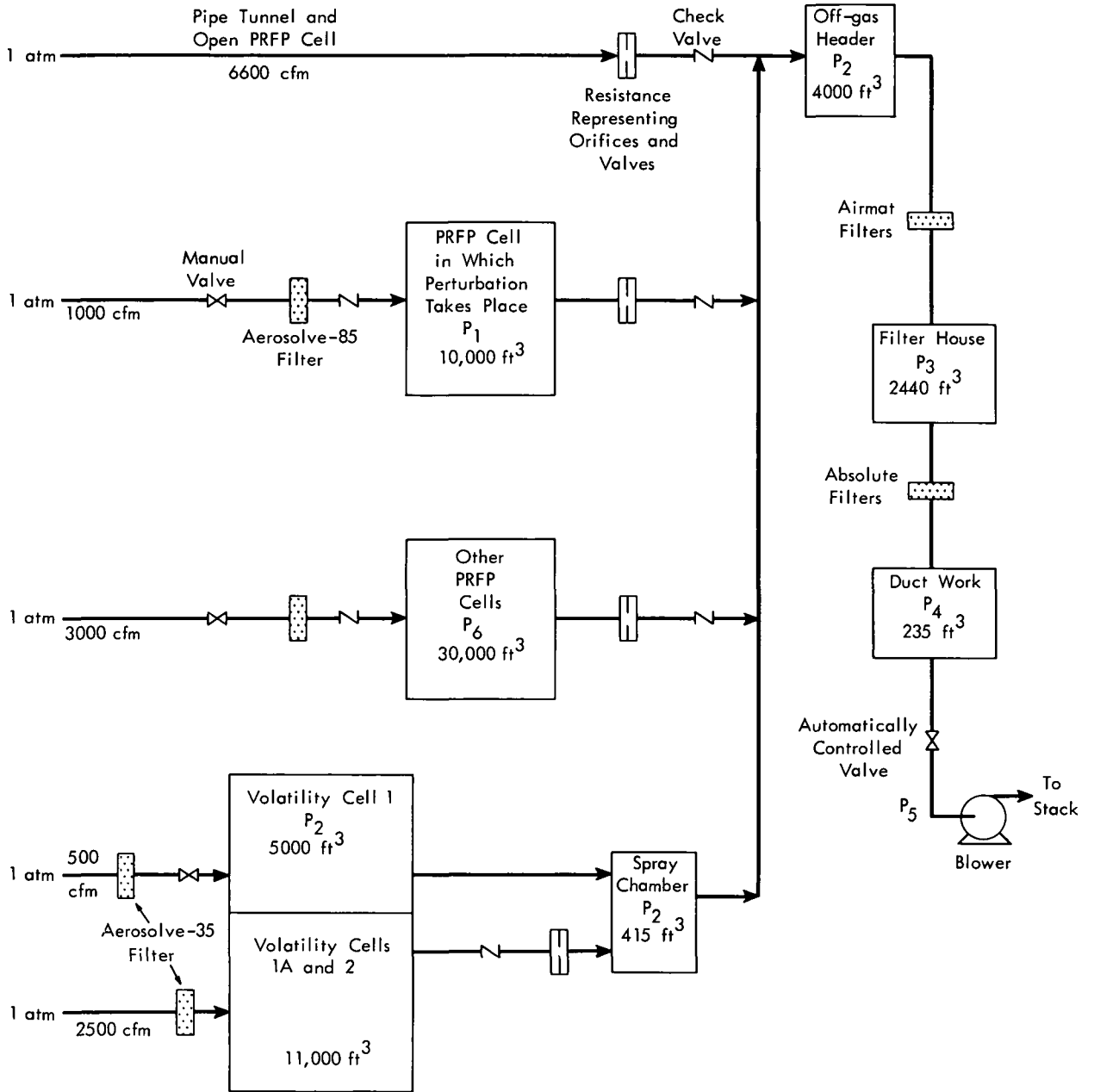


Fig. 1. Schematic of cell ventilation system in Bldg. 3019.

Table 1. Resistances of Valves, Orifices, and
Filters in Cell Off-gas System

<u>Valves</u>	<u>Resistance</u>
Inlet to cell P ₁	28.7 (in. H ₂ O) ^{1/2} /(lb-moles/sec)
Inlet to combined cells P ₆	9.57
Automatically controlled valve	6.24
 <u>Orifices</u>	
Outlet of cell P ₁	6.22 (in. H ₂ O) ^{1/2} /(lb-moles/sec)
Outlet of cell P ₆	2.07
Combined resistances of valve from pipe tunnel, orifice from open PRFP cell, valve in inlet to Volatility cell 1, orifice in outlet of Volatility cells 1A and 2	2.98
 <u>Filters</u>	
Airmats combined	0.511 (in. H ₂ O)/(lb-moles/sec)
Absolutes combined	1.30

The resistances of the Aerosolve-85 filters and the Aerosolve-35 filter in the inlet to Volatility cell 1 were negligible compared to those of the manual valves in series with them. Since the pressure drop through the Aerosolve-35 filter in the inlet to Volatility cells 1A and 2 would be only about 0.2 in. H₂O, the filter was neglected and the cells were treated as if open to the atmosphere. Several streams were treated as a single stream because they entered from the atmosphere into the same capacitance in the system, passing through orifices or valves which obey the same flow rate—pressure drop equation.

The volumes of the filter house and the ductwork between the filter house and the blower are small compared to other capacitances in the system, and are separated from the sites of the perturbations by orifices and filters; hence the accumulation terms in these capacitances were assumed to be negligible. Because of the negligible pressure drop in the ductwork, the volumes of Volatility cell 1, the spray chamber, and the off-gas header act as a single capacitance. The automatically controlled valve had not yet been designed at the time the calculations were made, and was assumed to be unaffected by the perturbations in the processing cells. In the light of the results of the calculations, this assumption was a good one because the perturbations were of only several seconds' duration for the impulse perturbations, and had very little effect on this part of the system in the case of ramp perturbations.

The blower in the system has a nominal rating of 22,000 cfm at 8.5 in. H₂O static head. A few points taken from the Chicago Blower Company catalog showed that over the narrow range of interest the blower capacity decreased proportionally to the square root of the head as predicted by the fan law (Fig. 2).

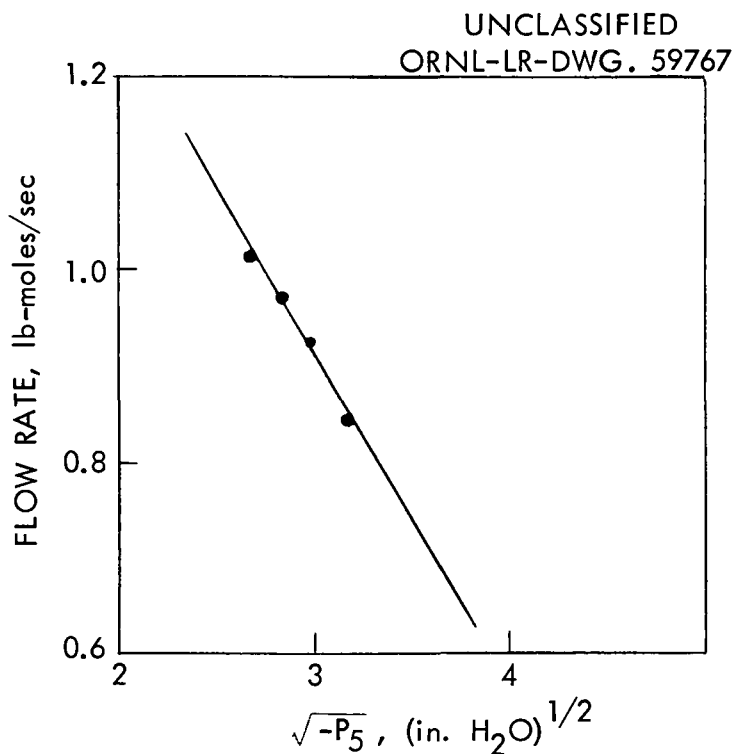


Fig. 2. Effect of head on capacity of blower at 3020 stack.

The equation used to represent these data is

$$Q = 1.89 - 0.329 \sqrt{-P_5} \quad (3-1)$$

where Q = flow rate, lb-moles/sec

P₅ = inlet pressure, in. H₂O

Having presented a description of the Bldg. 3019 ventilating system and the assumptions made about its operation, the following equations can be set down:

$$\frac{dP_1}{dt} = 0.545 \sqrt{-P_1} - 2.52 \sqrt{P_1 - P_2} \quad (3-2)$$

$$\frac{dP_6}{dt} = 0.545 \sqrt{-P_6} - 2.52 \sqrt{P_6 - P_7} \quad (3-3)$$

$$\text{with } P_7 = P_2 \text{ when } P_2 < P_6 \quad (3-4)$$

$$P_7 = P_6 \text{ when } P_2 \geq P_6 \quad (3-5)$$

$$dP_2/dt = 5.57 \sqrt{-P_2} + 2.67 \sqrt{P_1 - P_2} + 8.02 \sqrt{P_6 - P_7} - 2.70(11.8 - 2.05 \sqrt{-P_5}) \quad (3-6)$$

$$P_2 = P_5 + (11.8 - 2.05 \sqrt{-P_5})^2 + 0.292 (11.8 - 2.05 \sqrt{-P_5}) \quad (3-7)$$

The relation in (3-4) simulates the action of the check valve at the outlet of the PRFP cells in which no perturbation takes place. As long as $P_2 < P_6$, the valve is open and flow takes place at a rate proportional to the square root of the pressure drop across the orifice located there; however, if $P_2 \geq P_6$, the output term in eq. 3-3 and inlet term in eq. 3-6 associated with flow through this duct are made to equal zero.

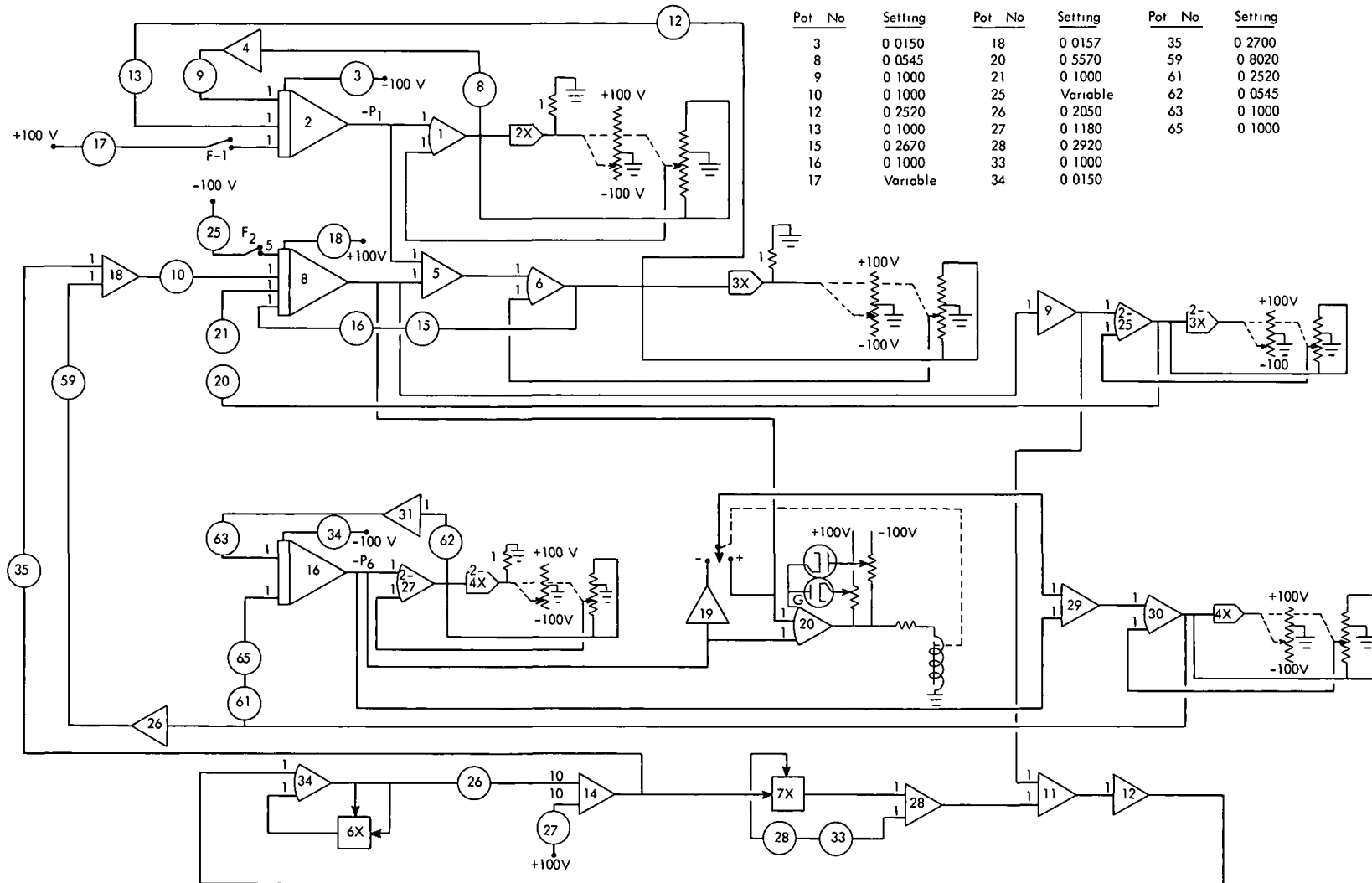
3.3 Analog Solution

A block diagram of the analog computer circuitry for the solutions of eqs. 3-2 through 3-7 is given in Fig. 3. The switching circuit associated with high-gain amplifier 20 simulates the check valve action of eqs. 3-4 and 3-5. With the potentiometer settings listed, 10 sec of machine time represents 1 sec of problem time.

Impulse perturbations were simulated by setting the initial condition on amplifier 2 (for perturbations to a PRFP cell) and amplifier 8 (for perturbations to Volatility cell 1) on other than steady-state values prior to switching the computer to the "operate" position. Ramp perturbations were introduced by closing switch F-1 or F-2 with the computer operating at steady state. Potentiometer settings 17 and 25 determined the magnitude of the ramp perturbations. After the effects of the ramp perturbations had been determined, switch F-1 or F-2 was opened and the recovery of the system was observed.

3.4 Results

Examples of the effects of impulse perturbations in a PRFP cell are shown in Figs. 4 and 5. For a perturbation of +8.0 in. H₂O, the cell returned to atmospheric pressure in 1.5 sec. No other points in the system exceeded atmospheric pressure. For a perturbation of +50.0 in. H₂O, the cell returned to atmospheric pressure in 4.7 sec. P_2 rose to a maximum of +1.1 in. H₂O. P_6 , having been cut off from the rest of the system by the closure of the check valve, drifted up toward atmospheric pressure, but reached a maximum of -0.2 in. H₂O before returning to its steady-state value. An example of an impulse perturbation in Volatility cell 1 is shown in Fig. 6. For a perturbation of +16.0 in. H₂O, the Volatility cell returned to atmospheric pressure in 0.55 sec. P_1 shows the effect of the perturbation on a PRFP cell if its outlet check valve did not seat. P_1 rose to a maximum of +1.2 in. H₂O and was above atmospheric pressure for 0.75 sec. P_6 shows the effect of the perturbation on PRFP cells whose outlet check valves did seat. P_6 rose to a maximum of -0.9 in. H₂O.



Pot No	Setting	Pot No	Setting	Pot No	Setting
3	0 0150	18	0 0157	35	0 2700
8	0 0545	20	0 5570	59	0 8020
9	0 1000	21	0 1000	61	0 2520
10	0 1000	25	Variable	62	0 0545
12	0 2520	26	0 2050	63	0 1000
13	0 1000	27	0 1180	65	0 1000
15	0 2670	28	0 2920		
16	0 1000	33	0 1000		
17	Variable	34	0 0150		

Fig. 3. Analog computer block diagram for cell ventilating system in Bldg. 3019.

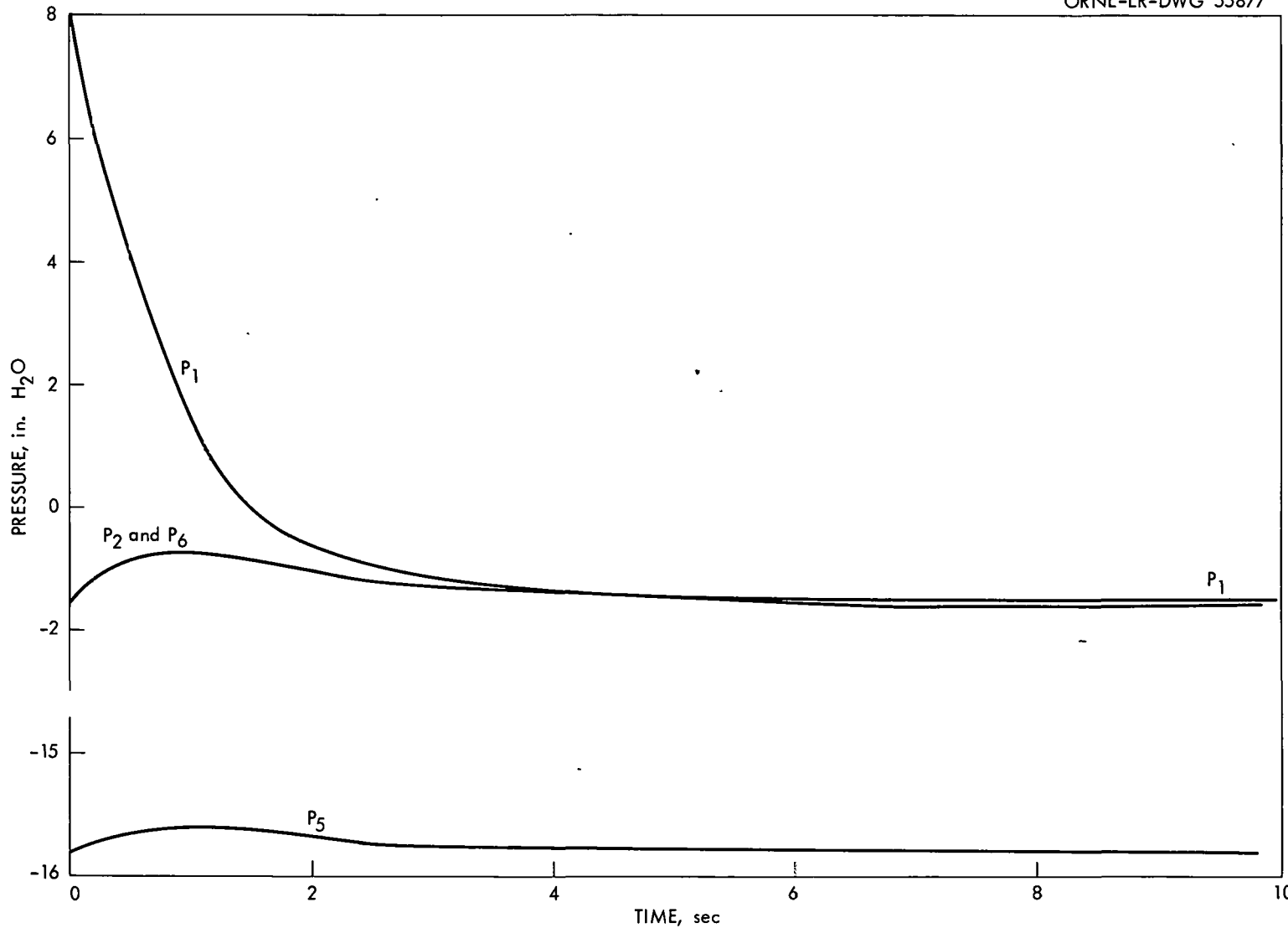


Fig. 4. Transient pressures in the ventilating system of Bldg. 3019 due to an impulse perturbation of +8.0 in. H₂O in a PRFP cell.

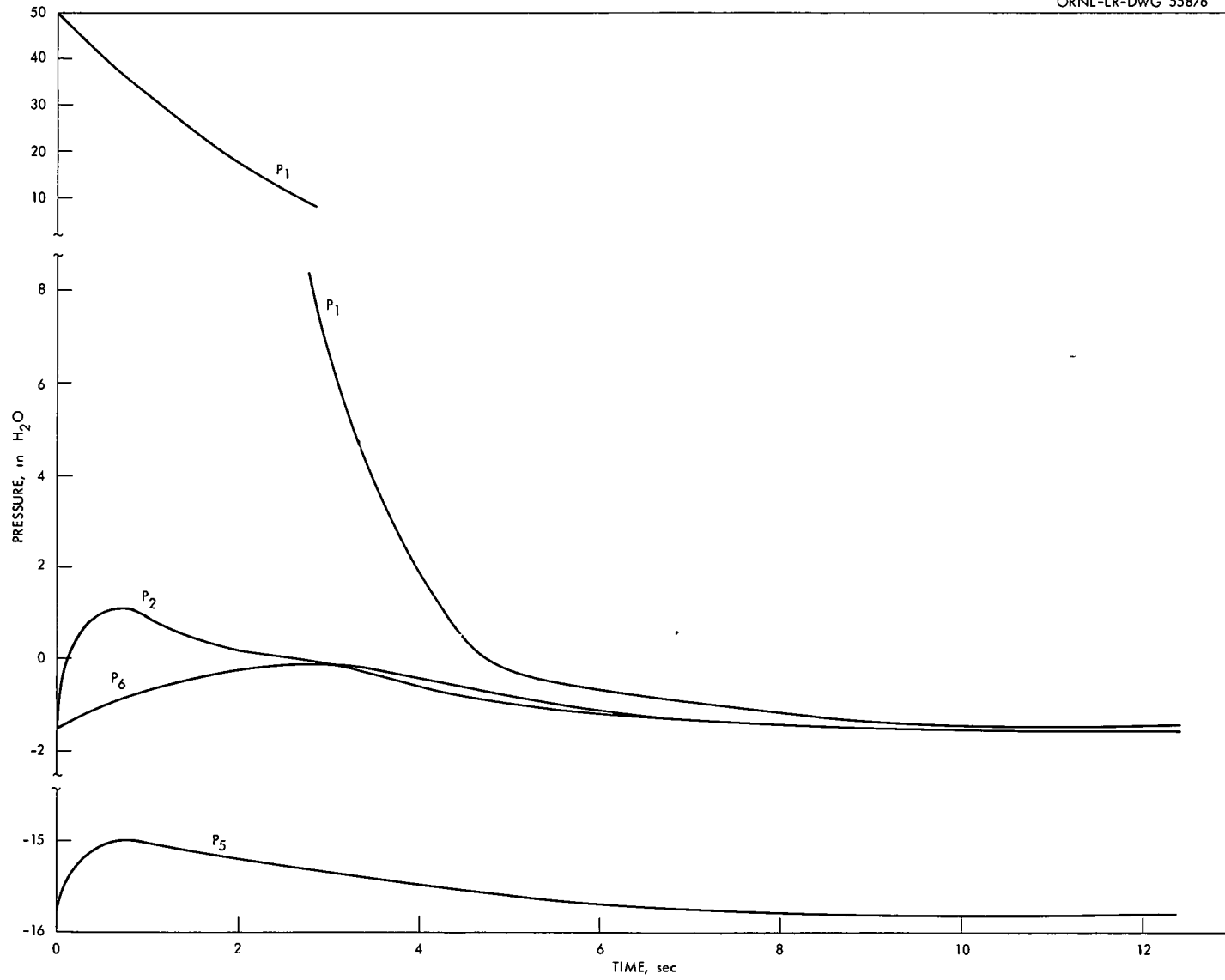


Fig. 5. Transient pressures in the ventilating system of Bldg. 3019 due to an impulse perturbation of +50 in. H₂O in a PRFP cell.

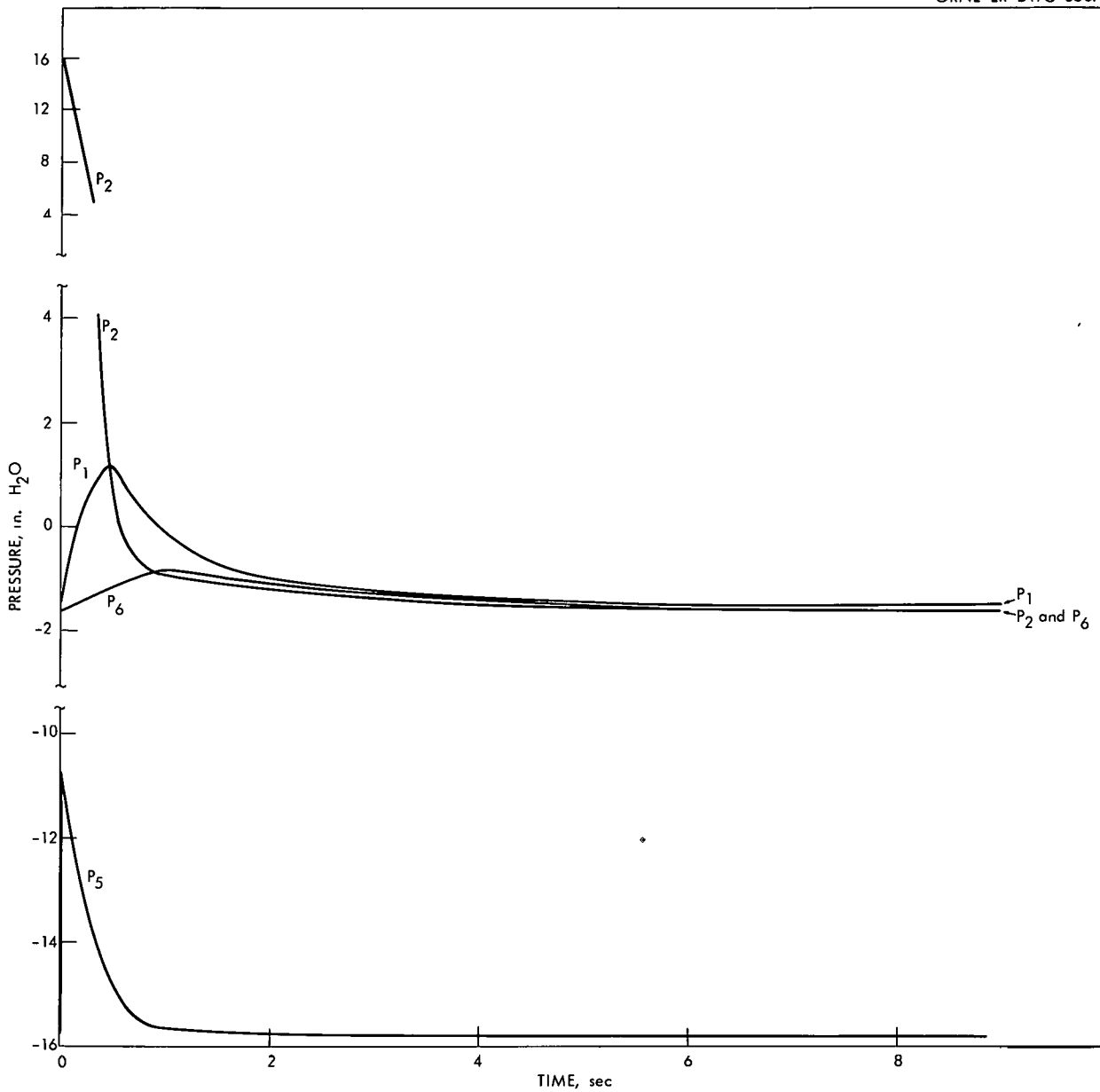


Fig. 6. Transient pressures in the ventilating system of Bldg. 3019 due to an impulse perturbation of ± 16 in. H₂O in Volatility cell 1.

In the calculations shown in Figs. 4, 5, and 6 the check valve at the inlet to the PRFP cell P_1 was not simulated. By using a switch in the circuit between potentiometer 9 and the input to integrating amplifier 2, the effect of the check valve in the impulse perturbations to the PRFP cell of +8.0 in. H_2O was found to be to increase the length of time required for P_1 to reach atmospheric pressure by 0.2 sec. Since the effect of the check valve was small, it was not simulated (i.e., the inlet was assumed to remain open throughout the calculation) in the rest of the cases studied.

An example of a ramp perturbation in a PRFP cell is shown in Fig. 7. A perturbation of 10 in. H_2O /sec caused P_1 to increase to +10.2 in. H_2O in 8.8 sec, at which point the switch F-1 was opened. P_1 dropped below atmospheric pressure in 1.8 sec after the perturbation stopped. At no other points in the system was atmospheric pressure exceeded.

Figure 8 shows an example of a ramp perturbation in Volatility cell 1. P_2 rose to a pressure of +8.7 in. H_2O in 7.2 sec due to a perturbation of 30 in. H_2O /sec. After cutoff, P_2 dropped below atmospheric pressure in 0.65 sec. The effect on a PRFP cell in which the outlet check valve does not close is shown by P_1 , which reached a maximum of +8.5 in. H_2O and required 2.1 sec to drop below atmospheric pressure.

Transient pressures in the filter house and the duct work immediately before the blower can be calculated from the following equations, used in the derivation of eq. 3-7:

$$P_2 - P_3 = 0.395(P_3 - P_4) \quad (3-8)$$

$$\sqrt{P_4 - P_5} = 11.8 - 2.05 \sqrt{-P_5} \quad (3-9)$$

From eq. 3-8 it can be seen that in order for P_3 to be greater than zero, $(P_2 + 0.395 P_4)$ must be greater than zero. From eq. 3-9 it can be shown that P_4 is larger than zero when P_5 is larger than -15.0 in. H_2O .

The time required for the cells in Bldg. 3019 to drop below atmospheric pressure following impulse perturbations as a function of impulse height is shown in Fig. 9. The response of the PRFP cells is much slower than that of Volatility cell 1 because the PRFP cells are separated from the blower by the capacitance of the Volatility cell. The minimum impulse perturbation to a PRFP cell which causes P_2 to exceed 1 atm is +25 in. H_2O . The minimum impulse perturbation in Volatility cell 1 that causes a PRFP cell to exceed 1 atm (if its outlet check valve fails) is +7.0 in. H_2O . If check valves seat, a perturbation to Volatility cell 1 cannot cause the pressure in a PRFP cell to exceed atmospheric pressure.

The results of the ramp perturbation calculations are summarized in Table 2. Ramp perturbations of 10 and 20 in. H_2O /sec to a PRFP cell would result in steady-state pressures in the cell of about +10.5 and 45 in. H_2O . A ramp perturbation of 10 in. H_2O /sec to Volatility cell 1 would raise its steady-state pressure to atmospheric.

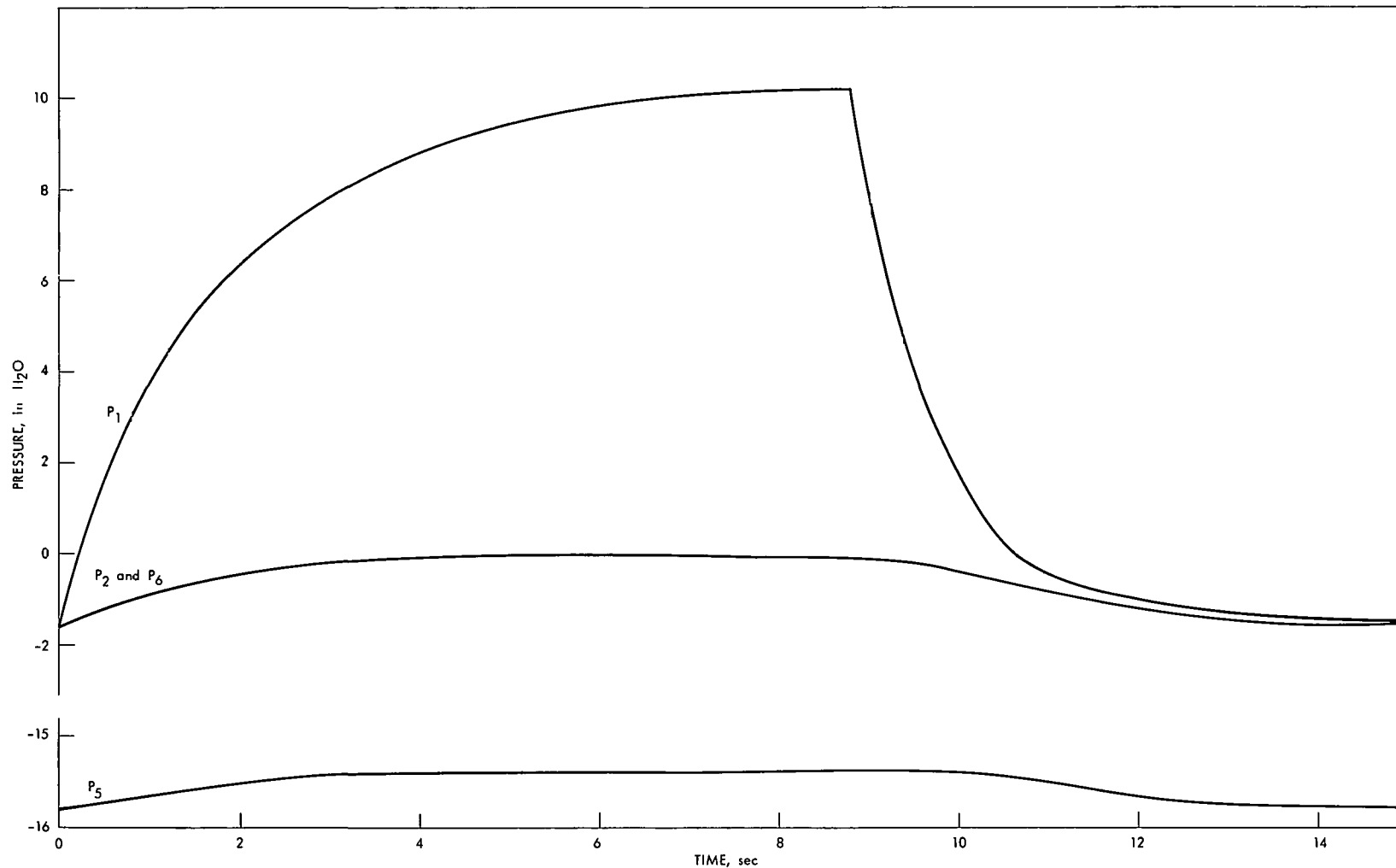


Fig. 7. Transient pressures in the ventilation system of Bldg. 3019 due to a ramp perturbation of 10 in. H₂O/sec in a PRFP cell.

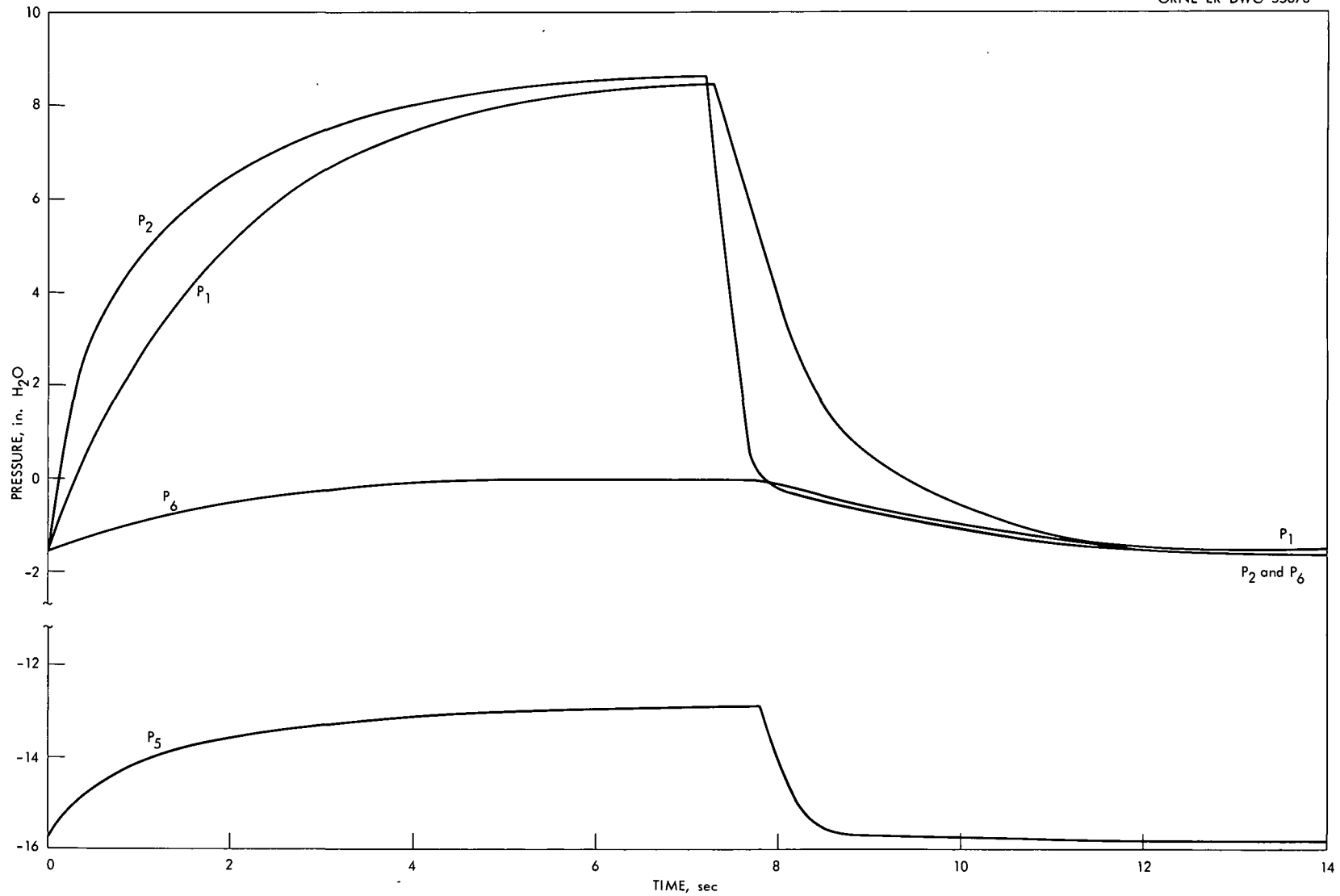


Fig. 8. Transient pressures in the ventilating system of Bldg. 3019 due to a ramp perturbation of 30 in. H₂O/sec in Volatility cell 1.

UNCLASSIFIED
 ORNL-LR-DWG. 59768

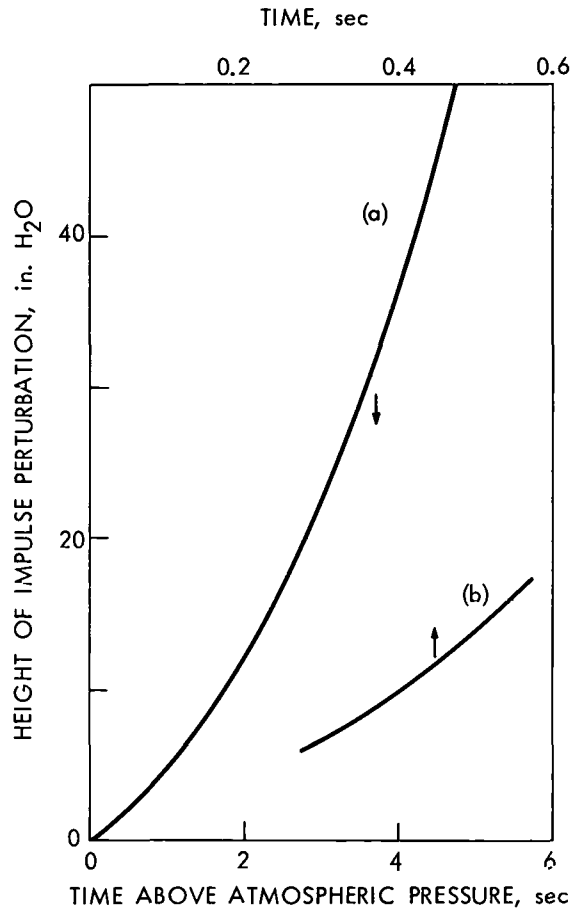


Fig. 9. Time required for PRFP and Volatility cells to drop below atmospheric pressure following impulse perturbations to (a) PRFP cell; (b) Volatility cell.

The outleakage can be calculated from eq. 2-4, using the permissible inleakage rate of 1% of the cell volume per minute under normal conditions to calculate a value for R_L . Leakage rates for each PRFP cell should not exceed 100 cfm and for Volatility cell 1 should not exceed 50 cfm at pressures $P_1 = -1.5$ in. H₂O and $P_2 = 1.57$ in. H₂O. Using these numbers, values for R_L are 0.735 (in. H₂O)^{1/2}/(ft³/sec) for a PRFP cell and 1.50 for Volatility cell 1. Applying eq. 2-4 to the data in Figs. 4 through 8, outleakages from the PRFP cell were calculated to be 3.1 ft³ and 17.0 ft³ for impulse perturbations of +8.0 and +50.0 in. H₂O, and 36.1 ft³ for the ramp perturbation of 10 in. H₂O/sec for 8.8 sec. Outleakages for Volatility cell 1 were calculated to be 0.88 ft³ for an impulse perturbation of +16.0 and 18.6 ft³ for a ramp perturbation of 30 in. H₂O/sec for 7.2 sec.

Table 2. Effects of Ramp Perturbations

Intensity, in. H ₂ O/sec	Length, sec	Max P ₁ , in. H ₂ O	Max P ₂ , in. H ₂ O	Total Time P ₁ above Atm Pressure, sec
PRFP Cells				
10	1.1	+4.2	-0.7	1.9
	2.4	+7.1	-0.2	3.6
	8.8	+10.2	-0.10	10.4
20	0.75	+8.2	-0.5	2.1
	1.1	+12.2	-0.2	3.0
	1.6	+16.3	0	3.9
	4.3	+30.0	+0.6	7.6
	16.7	+43.0	+1.4	20.9
Volatility Cell 1				
10	4.0	+0.5	0	2.6
20	6.7	+2.5	+2.4	6.8
30	7.2	+8.5	+8.7	7.7
50	1.4	+8.0	+16.9	2.1

4.0 CELL VENTILATION SYSTEM IN BLDG. 3026

4.1 Description of Ventilating System

A representation of the cell ventilation system of Bldg. 3026 is shown schematically in Fig. 10.

The maintenance facility, located above cells A and B, the charge room, and the discharge room, serves as the secondary containment area. A negative pressure of -0.2 in. H₂O will be maintained in this area by a pressure controller which operates five sets of inlet dampers, each drawing air from outside the area through a roughing filter and backflow preventer. During normal cell A operations the by-pass duct from the maintenance facility will be closed. If, however, during nonroutine operations, personnel must have access to the maintenance facility, a flow of approximately 4000 cfm will be maintained through the maintenance facility via the by-pass duct. This flow will be sustained by a flow controller, which uses a pitot-tube sensing element to operate an automatic damper valve in this duct.

UNCLASSIFIED
ORNL-LR-DWG 55872

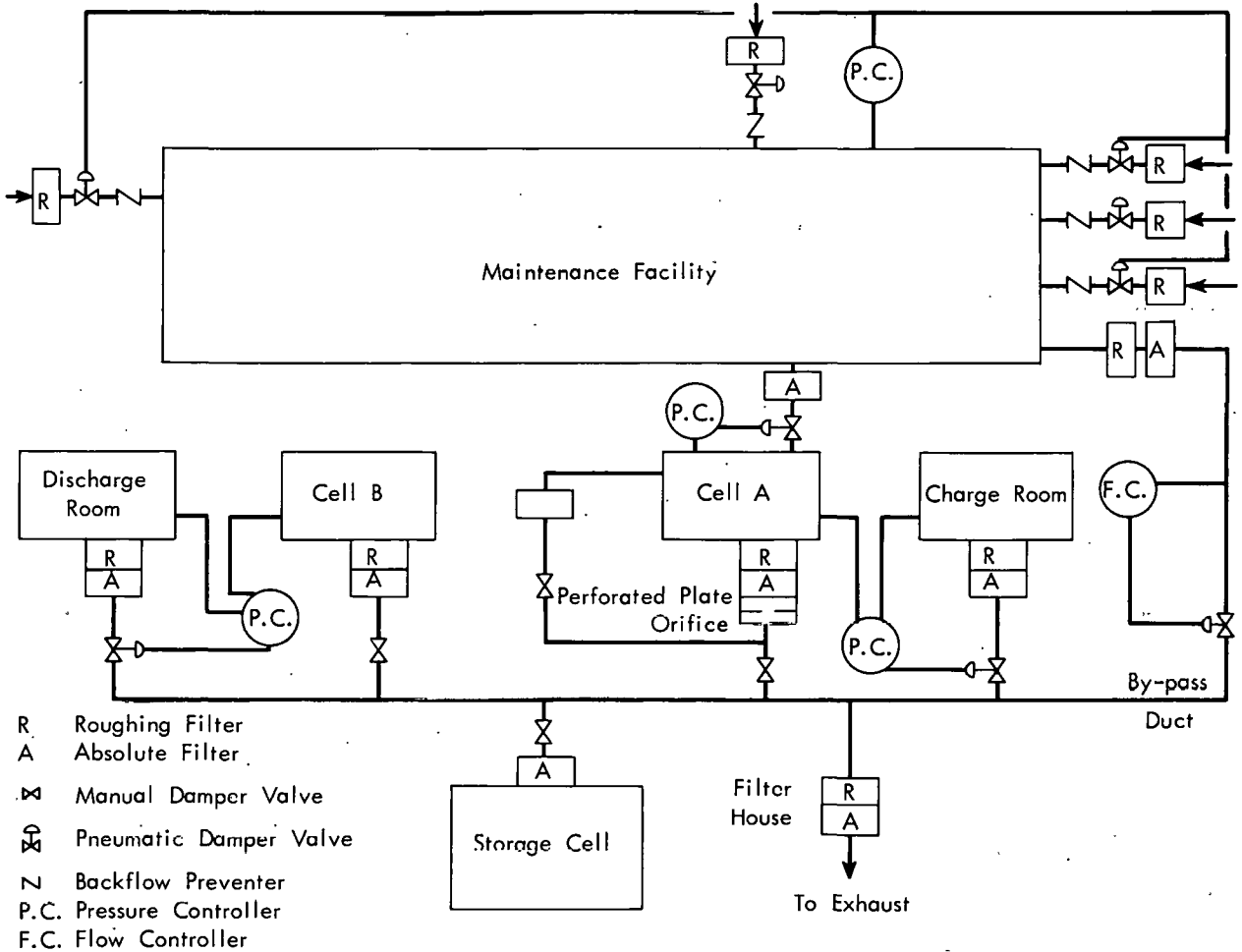


Fig. 10. Schematic diagram of Bldg. 3026 cell ventilation system.

In addition to inflow through the five inlets provided to the facility, there will be an air leakage through cracks and crevices in the walls. Although there is no rational way of predicting this leak rate, the estimated value of 500 cfm at a pressure drop of 0.2 in. H₂O is thought to be the most realistic.

Cell A is the main process cell in which mechanical decladding and chopping operations can be performed, for example, on NaK-clad SRE assemblies. Thus it appears that cell A would be the most likely place for a pressure incident to occur.

A modulated air flow enters the cell from the maintenance facility through a duct containing four 24- by 24- by 11.5-in. absolute filters in parallel. These filters were installed to remove any air-borne activity, which would otherwise be blown back into the secondary containment area if the flow pattern should reverse as a result of a pressure surge. Cell A pressure will be controlled to -1.0 in. H₂O by a General Regulator Corporation two-blade opposed-motion damper operated by a Johnson Service Company type R-317 proportional controller. The damper, located on the cell inlet, is provided with a valve positioner and 90 psi supply which amplifies the 3 to 15 psi signal from the controller to actuate a bellows chamber. Air failure causes the damper to close. The R-317 is a nonadjustable proportional controller requiring a 20-psi supply and has a sensitivity of 3 psi/0.01 in. water gage error signal.

Normal air exhaust from the cell is through a roughing filter, absolute filter, perforated plate orifice, and manual damper valve. At this point the duct ties into the main exhaust header from the other cells where the entire flow is passed through a final bank of roughing and absolute filters. A small side stream of approximately 150 cfm is continuously withdrawn from the ceiling of cell A, which is for the purpose of sweeping the top of the cell clear of any H₂ that may accumulate as a result of an accidental water reaction with NaK.

The actual steady-state flow rate through cell A is expected to be the lowest rate that maintains the ambient cell temperature at a reasonable value. An inleakage rate of 250 cfm at -1.0 in. H₂O appears to be the best available estimate. For purposes of analysis, it will be assumed that the 250 cfm inleakage plus a modulated flow of 500 cfm will be adequate to prevent the cell A temperature from becoming too high. This assumption simplifies the dynamic analysis considerably because the entire flow into the maintenance facility would be through inleakage, requiring no flow through the five damper inlets. Actually, if this were not the case, results would not be seriously impaired by this approach because small pressure transients in the maintenance facility have only a minor effect on cell A pressure, and it is the cell A pressure that is of primary concern.

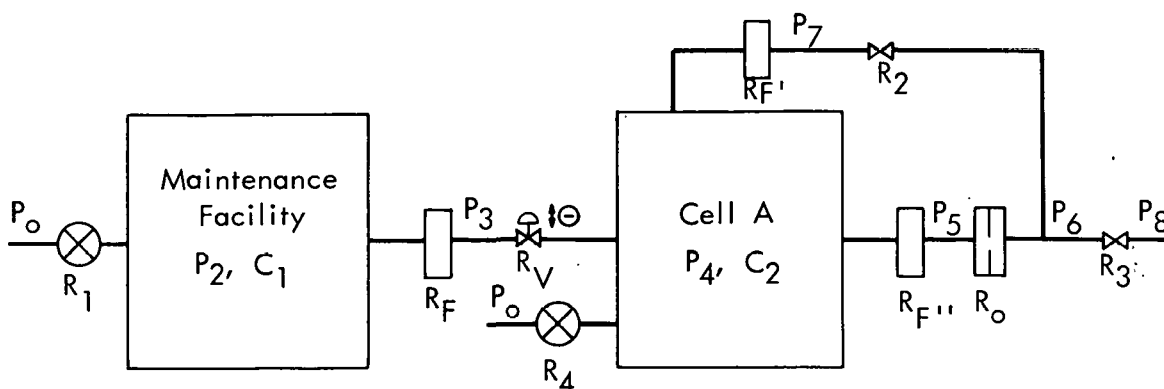
Cell B, the charge room, the discharge room, and the storage cell rely entirely on inleakage for flow. Differential pressure controllers operate dampers on the charge and discharge rooms so that these pressures will be above those of cells A and B, respectively.

The available suction from the fan at the stack is about -7.75 in. H₂O. The pressure drop across the final bank of filters is negligible, so that the gage pressure in the exhaust header may be assumed a constant -7.75 in. H₂O.

Immediately downstream of the filter house the Bldg. 3026 exhaust header joins the exhaust header from Bldg. 3025. Currently, a 60,000 cfm capacity blower operating at about half capacity supplies the vacuum for the cell ventilation systems of Bldgs. 3025 and 3026. A rough estimate of the volume of ductwork in this main header leading to the fan at the 3039 stack indicated at least 2500 ft³. The maximum impulse perturbation simulated would release about 5 ft³ of air to this duct during the first second. If this volume of air should be released instantaneously, the resulting pressure rise in the duct to the fan would be only about 0.8 in. H₂O. Actually, the release is not instantaneous, and as soon as the fan sees the pressure rising it increases the flow, which in turn decreases the accumulation in the duct. Thus the assumption of constant pressure in the duct is justified.

4.2 Mathematical Treatment and Analog Circuit Development

The Maintenance Facility and cell A flow scheme, broken down into pure resistance and capacitances, may be diagrammed:



The capacities, resistances, steady-state flow rates, and pressures in Bldg. 3026 are:

Maintenance Facility volume
Cell A volume

19,800 ft³
3,190 ft³

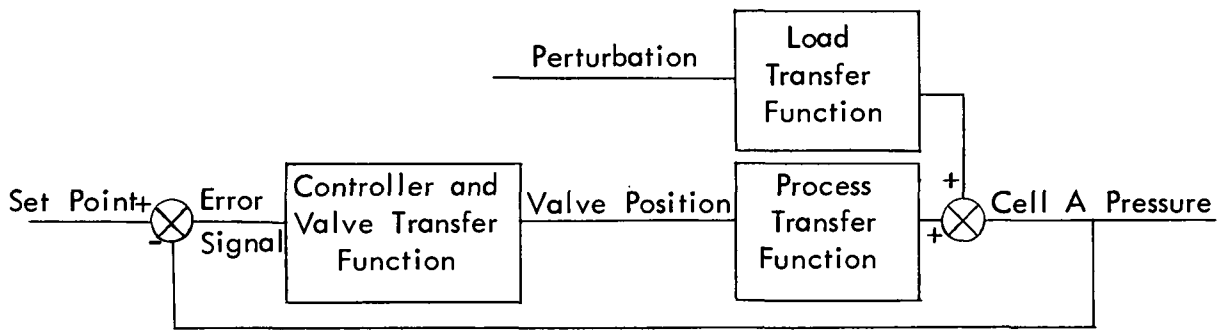
Resistance per cfm
(in. H₂O)^{1/2} in. H₂O

R ₀ Orifice plate	0.00301	
R ₁ Maintenance Facility leakage	0.00089	
R ₂ Ceiling sweep exit valve	0.01190	
R ₃ Final reduction valve	0.00230	
R ₄ Cell A leakage	0.00400	
R _F Cell A inlet filters		0.00023
R _{F'} Ceiling sweep exit filter		0.00410
R _{F''} Cell A exhaust filters		0.00091

	Steady-state Flow Rates, cfm
q ₁ Maintenance Facility inleakage	500
q ₂ Modulated cell A flow	500
q ₃ Cell A inleakage	250
q ₄ Ceiling sweep	150
q ₅ Cell A exhaust	600
q ₆ Total cell A discharge	750

	Steady-state Pressures, in. H ₂ O
P ₀	0
P ₂	-0.200
P ₃	-0.313
P ₄	-1.000
P ₅	-1.545
P ₆	-4.81
P ₇	-1.612
P ₈	-7.75

The control-loop block diagram is shown schematically as:

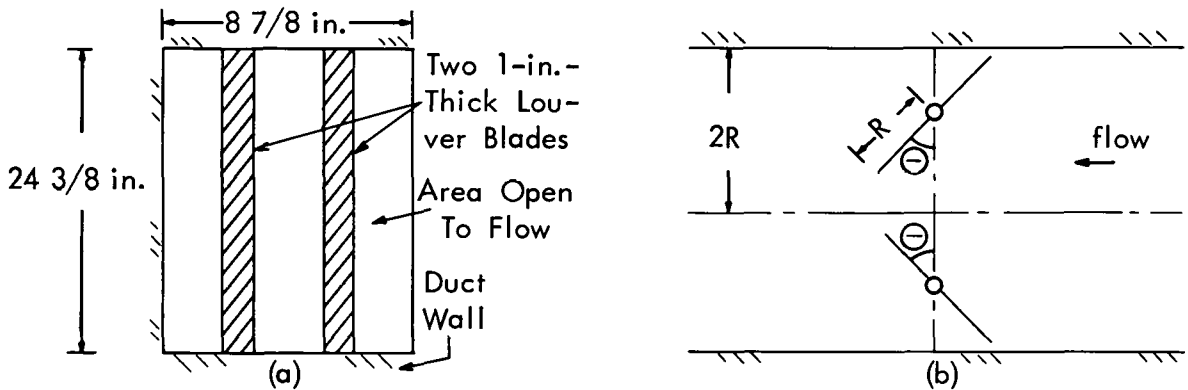


The process transfer function may be derived indirectly by a series of non-steady-state air material-balance equations about cell A and the Maintenance Facility.

The Maintenance Facility material balance reduces to

$$\frac{dP_2}{dt} = \frac{RT}{C_1} \left(\sqrt{\frac{P_0 - P_2}{R_1}} - \frac{P_2 - P_3}{R_F} \right) \quad (4-1)$$

Flow through the automatic damper valve on the cell A inlet was treated by the orifice equation with a variable orifice coefficient. Views of the damper valve (a) along the direction of flow with the two louver blades in the full-open position and (b) from the side with the two-blade damper rotated to angle θ with a louver blade width of $2R$ may be shown as:



For any valve position, flow through the valve may be represented by

$$Q = f \sqrt{P_3 - P_4} / R_V \quad (4-2)$$

where f = fraction of the total duct cross sectional area open to flow.

When the two louver blades are fully closed ($\theta = 0$), the duct is completely restricted to flow. There is no overlapping of the blades, so that the cross sectional area perpendicular to flow based upon unit duct width is

$$A = 4R(1 - \cos \theta) \quad (4-3)$$

and the total duct cross section is

$$A_T = 4R \quad (4-4)$$

Thus

$$f = A/A_T = \frac{4R(1 - \cos \theta)}{4R} = (1 - \cos \theta) \quad (4-5)$$

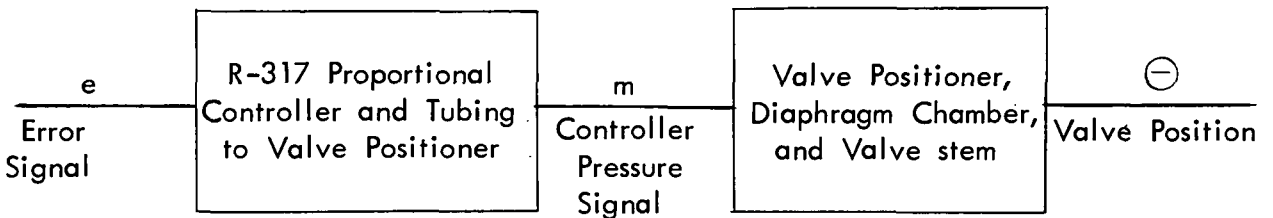
Information supplied by the Johnson Service Company based on experimental tests tends to support this type of valve characteristic representation for opposed-motion louver dampers.

The overall relation for flow through the valve may now be obtained by substituting eq. 4-5 into 4-2:

$$Q = (1 - \cos \theta) \sqrt{P_3 - P_4} / R_V \quad (4-6)$$

A steady-state valve position of 31.3° was calculated from eq. 4-6, using the steady-state flow rate and pressure drop.

The valve position, θ , is a function of cell A pressure, P_4 , since the valve is the final control element in the cell A pressure control loop. Experience has shown that the recovery time from pressure perturbations is very rapid. Process time constants are small enough that the response of the control loop cannot be assumed instantaneous, as is often done in process control analysis. The open-loop block diagram of the controller and valve may be shown as:



An error signal, e , induced in the controller results in a 3- to 15- psi pressure signal, m , which is transmitted through a length of 1/4-in. tubing to the valve positioner. This ultimately results in a valve position. In order to obtain the transfer functions of those two elements shown, a rather precise knowledge of the construction of the controller and valve positioner would be required. Such information was not available, so an experimental technique was used to obtain empirical transfer functions.

An experiment diagrammed in Fig. 11 was assembled. A 20-psi air supply to the controller and a 100-psi supply to the valve positioner was maintained throughout the experiment. Pressure gages were installed on the supply to the controller and the air signal from the controller. The signal to the valve positioner was recorded on a Sanborn recorder by a Compu-Tran 0- to 15-psig pressure transducer connected immediately downstream of the controller. Valve position was also recorded on the Sanborn by the slide wire resistor circuit. Differential pressure taps were left open to the atmosphere, and the set point of the controller was adjusted to give a signal in the 3- to 15-psig range. A step change in error signal was then simulated by quickly readjusting the set point. Controller signal and valve position were recorded simultaneously. Immediately after the set point had been readjusted, both the controller signal and valve position approached a final value in what appeared to be a simple time constant response.

UNCLASSIFIED
ORNL-LR-DWG. 59769

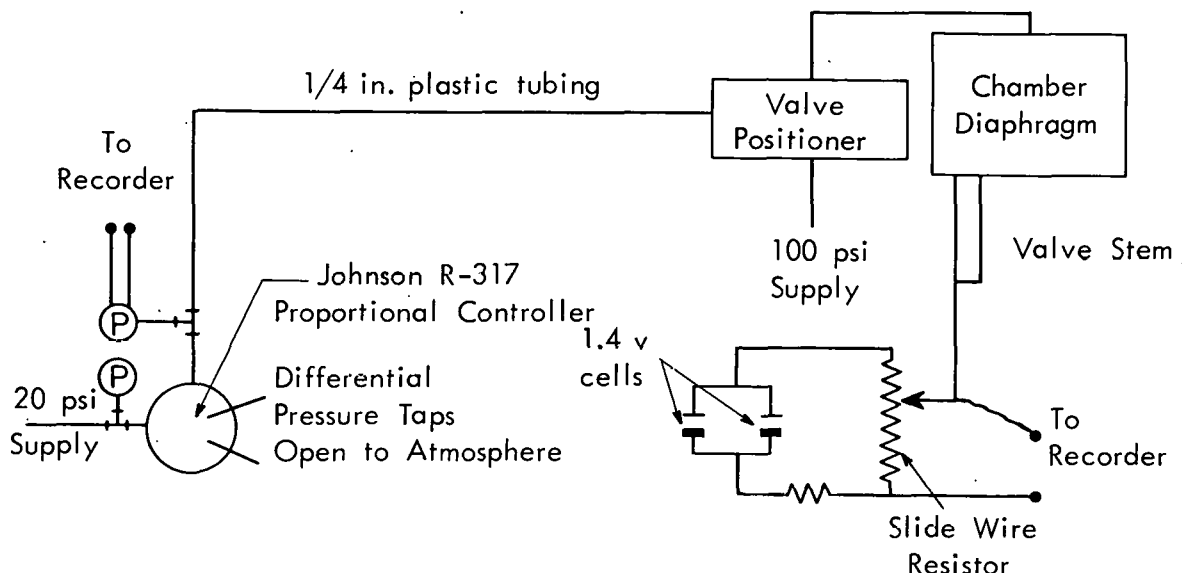


Fig. 11. Apparatus diagram for valve response experiments.

In fact, the response of the signal and valve position appeared to be identical. In other words, after a given time had elapsed since the set point was readjusted, both recorded variables reached essentially the same percentage of their final value. This leads to the conclusions that the time lag may be attributed entirely to the capacitance of the 1/4-in. tubing leading to the valve positioner, and that there is essentially no resistance to flow in this line.

Several runs were completed with stepping of the error signal in both directions (Table 3). One set was made with 28.6 ft of 1/4-in. tubing, another with 64.3 ft.

Assuming a time constant type response, time constants for each run were computed directly by reading the time axis corresponding to a valve position of 63.2% ($1 - 1/e$) of its final value. Two time constants were observed, one for air flowing through the controller and opening the valve and a smaller one for air bleeding from the transmission line and closing the valve. The averaged time constants for opening and closing the valve with 28.6 ft of tubing were 9.4 and 4.3 sec, respectively. When 64.3 ft of tubing was used, the time constants increased to 17.1 and 9.1 sec. Results of two typical runs are plotted in Fig. 12 alongside the curves predicted by the averaged time constants. The fact that the curves tend to coincide indicates that the response is well indicated by the characteristic exponential approach of the time constant.

UNCLASSIFIED
ORNL-LR-DWG 55883

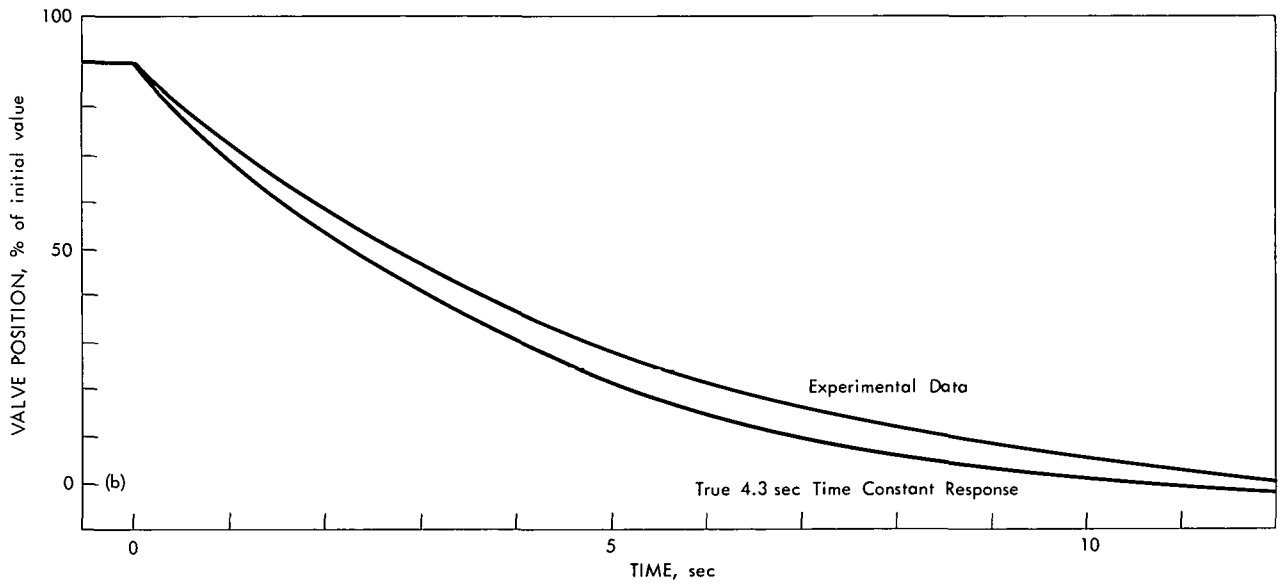
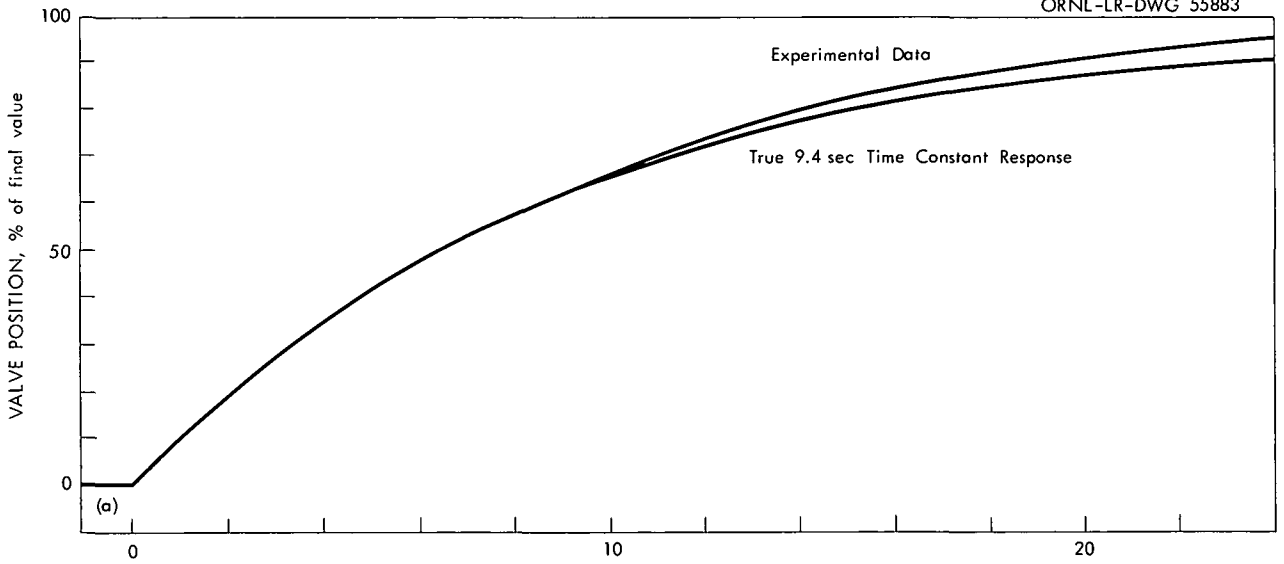


Fig. 12. Response of (a) opening valve (run 5) and (b) closing valve (run 7) to step change in error signal with 28.6-ft. tubing from controller to positioner.

Table 3. Controller and Valve Response to Step Changes in Error Signal

Run No.	Initial Valve Position, % open	Final Valve Position, % open	Direction of Change	Time for Controller Signal to Reach 63.2% of Final Value, sec	Time for Valve Position to Reach 63.2% of Final Value, sec	Length of Tubing from Controller to Valve, ft
1	0	100	Open	10.4	10.9	28.6
2	70.0	0	Close	3.9	3.9	
3	20.0	85.0	Open	8.8	8.8	
4	85.0	23.8	Close	5.2	5.4	
5	0	97.5	Open	-	9.3	
6	75.0	0	Close	-	3.7	
7	75.0	31.3	Close	-	5.2	
8	31.3	95.0	Open	-	8.4	
9	47.5	0	Close	-	3.1	
10	67.5	0	Close	-	6.8	64.3
11	37.5	75.0	Open	-	13.9	
12	75.0	5.0	Close	-	8.6	
13	15.0	90.0	Open	-	17.8	
14	90.0	0	Close	-	12.0	
15	57.5	5.0	Close	-	8.8	
16	5.0	90.0	Open	-	18.2	
17	100	0	Close	-	5.4 ^a	
18	0	100	Open	-	18.4	

^aRun 17 omitted from calculations

After these data had been collected, it was decided to locate the controller as near the valve as possible so that the fastest response would be realized. This would require approximately 5 ft of transmission line. A linear extrapolation of the experimental time constants to 5 ft of tubing yields time constants of 4.3 and 1.1 sec for opening and closing the valve. Linear extrapolation is justifiable in the sense that the capacitance (volume) of the tubing is directly proportional to the length, whereas the resistance to flow associated with the tubing is negligible.

A plot of steady-state valve position vs the steady-state controller signal is given in Fig. 13.

The transient material balance on cell A reduces to

$$\frac{dP_4}{dt} = \frac{RT}{C_2} \left[\frac{(1 - \cos \theta) \sqrt{P_3 - P_4}}{R_V} + \frac{\sqrt{P_0 - P_4}}{R_4} - \frac{P_4 - P_7}{R_{F'}} - \frac{P_4 - P_5}{R_{F''}} \right] \quad (4-7)$$

UNCLASSIFIED
ORNL-LR-DWG 55878

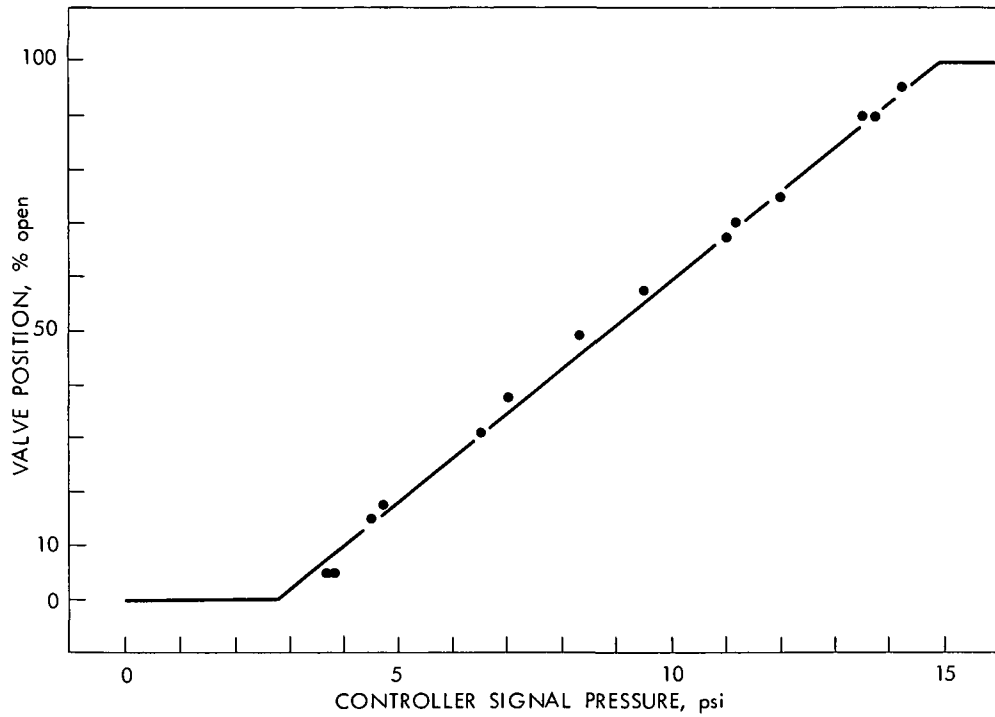


Fig. 13. Valve position as a function of controller signal pressure. Inlet to cell A in Bldg. 3026.

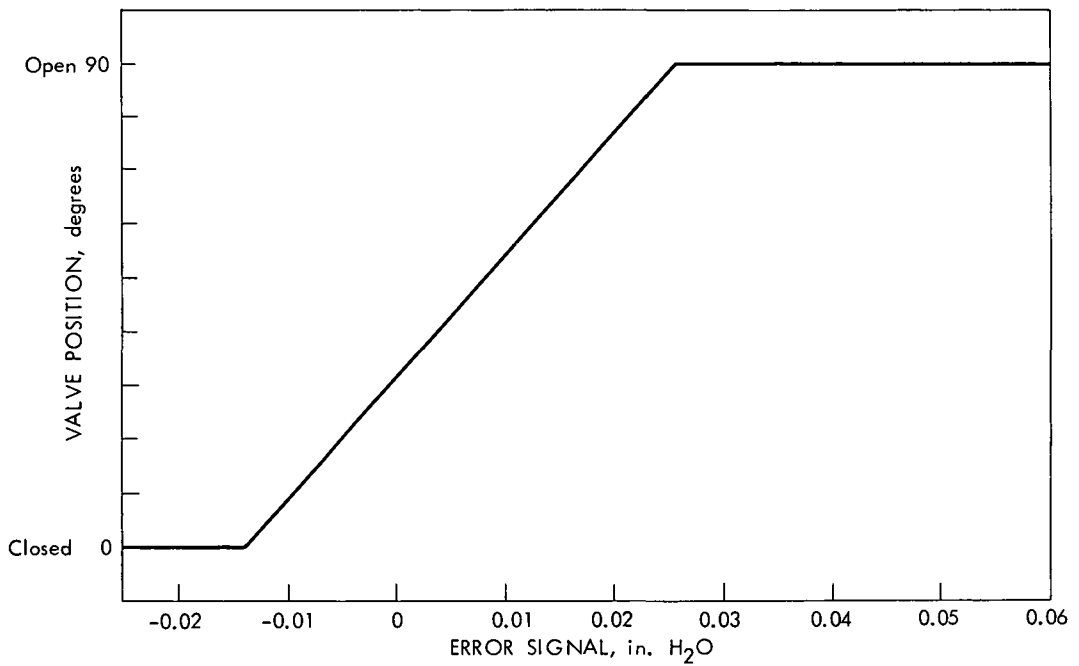


Fig. 14. Steady-state valve position as a function of error signal. Inlet to cell A in Bldg. 3026.

and since there is no capacitance effect associated with P_5 and P_7 ,

$$\frac{P_4 - P_7}{R_{F'}} = \frac{\sqrt{P_7 - P_6}}{R_2} \quad (4-8)$$

$$\frac{P_4 - P_5}{R_{F''}} = \frac{\sqrt{P_5 - P_6}}{R_0} \quad (4-9)$$

Finally, assuming no capacitance effect associated with P_6 ,

$$\frac{P_4 - P_5}{R_{F''}} + \frac{P_4 - P_7}{R_{F'}} = \frac{\sqrt{P_6 - P_8}}{R_0} \quad (4-10)$$

Substitution of numerical values into the foregoing group of relations yields:

for eq. 4-1

$$\frac{dP_2}{dt} = 0.410\sqrt{-P_2} - 1.615(P_2 - P_3) \quad (4-11)$$

for eq. 4-7

$$\frac{dP_4}{dt} = 1.002(P_2 - P_3) + 0.5683\sqrt{-P_4} - 0.5583(P_4 - P_7) + 2.500(P_4 - P_5) \quad (4-12)$$

for the inlet line to cell A

$$P_3 = P_2 - 0.945(1 - \cos \theta) \sqrt{P_3 - P_4} \quad (4-13)$$

for eq. 4-8

$$P_7 = P_4 - 0.343 \sqrt{P_7 - P_6} \quad (4-14)$$

for eq. 4-9

$$P_5 = P_4 - 0.302 \sqrt{P_5 - P_6} \quad (4-15)$$

for eq. 4-10

$$P_6 = [2.52(P_4 - P_5) + 0.562(P_4 - P_7)]^2 + P_8 \quad (4-16)$$

Analog variables were defined as:

Real variable, in. H ₂ O	P_2	P_3	P_4	P_5	P_6	P_7	P_8
Equivalent analog variables, volts	$Z_2/100$	$Z_3/100$	$Z_4/10$	$Z_5/10$	$Z_6/10$	$Z_7/10$	$Z_8/10$

Substitution of the new variables into eqs. 4-11 through 4-16 and dividing the right-hand sides of eqs. 4-11 and 4-15 by 10 so that 10 machine seconds is equivalent to 1 real second gives

$$\frac{dZ_2}{d\tau} = 0.411 \sqrt{-Z_2} - 0.1615(Z_2 - Z_3) \quad (4-17)$$

where τ = machine time, seconds

$$\frac{dZ_4}{d\tau} = 0.100(Z_2 - Z_3) + 0.180 \sqrt{-Z_4} - 0.0558(Z_4 - Z_7) - 0.250(Z_4 - Z_5) \quad (4-18)$$

$$Z_3 = Z_2 - 9.45(1 - \cos \theta) \sqrt{Z_3 - 10Z_4} \quad (4-19)$$

$$Z_7 = Z_4 - 1.082 \sqrt{Z_7 - Z_6} \quad (4-20)$$

$$Z_5 = Z_4 - 0.954 \sqrt{Z_5 - Z_6} \quad (4-21)$$

$$Z_6 = [0.799(Z_4 - Z_5) + 0.178(Z_4 - Z_7)]^2 - 77.5 \quad (4-22)$$

The system has been reduced to six Z unknowns and θ , to make a total of seven unknowns. Defining the controller response will then complete the array of seven independent relations. A proportional controller in series with a time constant element (transmission line) may be represented in the differential form:

$$T \frac{d\theta}{dt} + \theta = K_c e \quad (4-23)$$

where θ = valve position, degrees

K_c = proportional sensitivity, 2250 degrees/in. H_2O error signal

e = error signal, in. H_2O

T = time constant (of tubing), sec

Since two time constants were observed experimentally, a switching circuit is required which will tell the analog machine to use the large time constant when the valve is opening or the smaller one when the valve is closing. The sign of the error signal was used to trigger the switching circuits.

For a step change in error signal, the open loop response of the controller is given by the solution to eq. 4-23:

$$\theta = \theta_0 + K_c e [1 - \exp(-t/T)] \quad (4-24)$$

where θ_0 = initial valve position

Equation 4-24 represents the experimental curves shown in Fig 12. Finally, it must be taken into account that the valve position **cannot exceed the range 0° to 90°** regardless of the extremes the error signal to the controller may reach.

The analog simulation of this limitation was attained by limiting the magnitude of the error signal with a pair of diodes, such that, starting at the steady-state position, no step change in error signal will rotate the

blades to greater than +90° nor less than 0° (Fig. 14). Circuitry was scaled so that the maximum value of cell A pressure that could be simulated without overloading the amplifiers was +10 in. H₂O. The final analog program is shown in Fig. 15. A listing of potentiometer settings is presented in Table 4. Tandem operation of the Reactor Controls Analog Facility was used for the simulation.

Table 4. Potentiometer Settings for Bldg. 3026 Program

Potentiometer			Potentiometer		
No.	Setting	Input	No.	Setting	Input
1	0.2000	-100	30	0.0140	
6	0.0411		31	0.494	
8	0.1615		32	0.791	
9	0.4420		33	0.2990	
10	0.1000		35	0.7990	
11	^a		36	0.0500	
12	0.1000	-100	39	0.7750	+100
14	0.5000		43	0.1000	-100
16	0.0180		44	0.1082	
22	0.3280	-100	51	0.0558	
23	0.0233 ^b		53	0.2180 ^b	
24	0.0910 ^b		54	0.7660 ^b	
26	0.1000		55	0.1780	
29	0.0260		58	0.0954	
			67	0.500	-100

^aPotentiometer 11 setting varied for ramp inputs.

^bSettings for potentiometers 23, 24, 53, and 54 decreased for runs 15 to 19.

Analog representation of the controller system made use of amplifiers 9, 10, 11, and 12 along with the resolver. The valve position, θ , was scaled directly as 1 volt per degree from the output of integrator 11. This was reduced 50% through potentiometer 14 because the resolver circuitry was scaled for 0.5 volt per degree. Diode limiters around amplifier 9 limited the error signal to potentiometers 53 and 54. The error signal was also amplified through high-gain amplifier 10 to trigger the switching circuit. Two switching circuits are available on board No. 1, each having two single-pole double-throw contacts. However, one was not working and only one pole of the remaining switch was making contact. The one pole that did work was used for potentiometers 53 and 54, and an external manual switch was used to contact either potentiometer 23 or 24 on the feedback around integrator 11. During operation the output of high-gain amplifier 10 was shown on the VTVM, indicating which contact should be made with the manual switch.

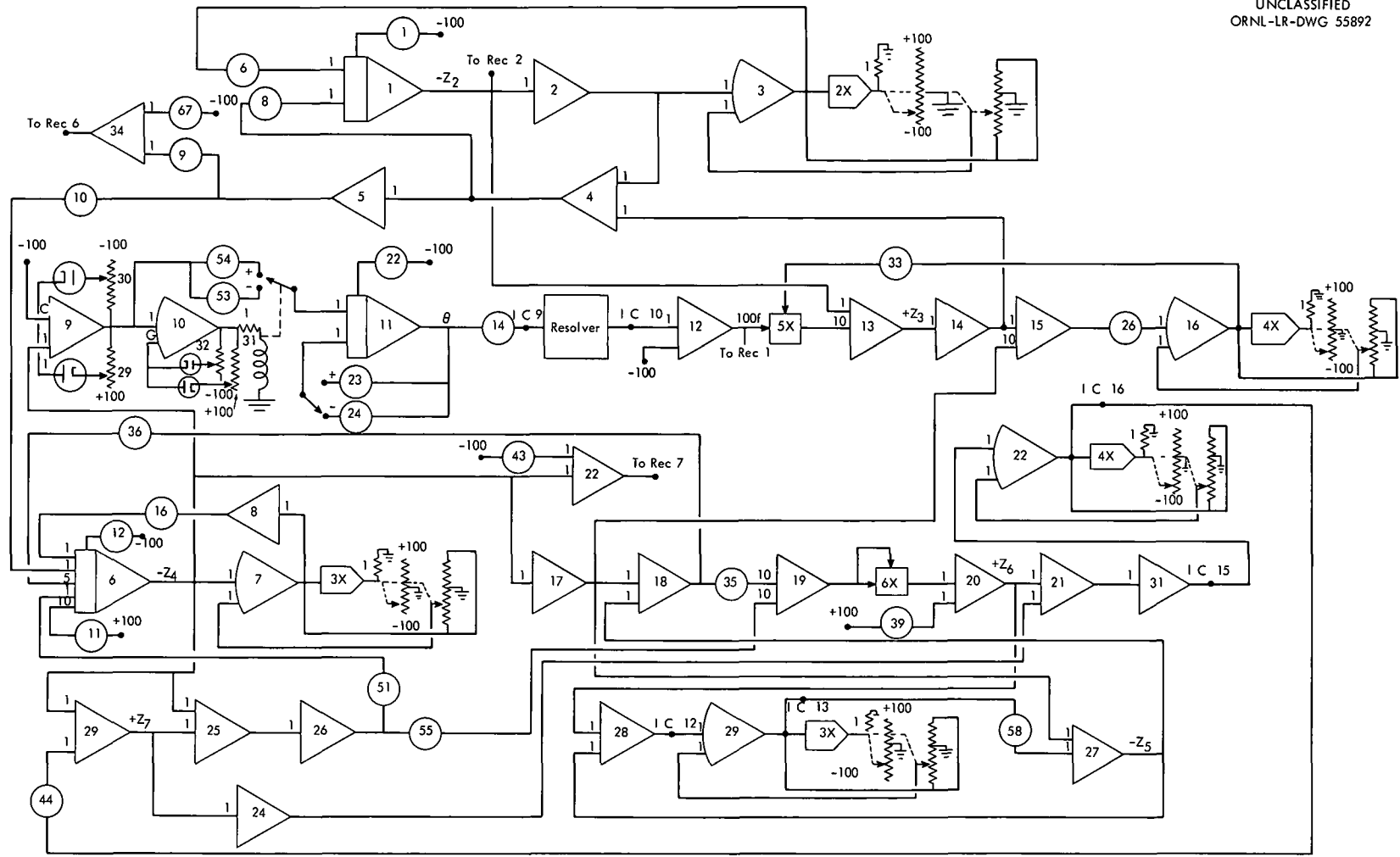


Fig. 15. Analog program, Bldg. 3026 cell ventilation simulation.

The quantity $100(1 - \cos \theta)$ was recorded on recorder 1. Integrator 1 represents the material balance about the Maintenance Facility, and the analog variable $-Z_2$ was shown on recorder 2. Cell A pressure was represented by the output of integrator 6, and this was wired to recorder 7. A plot of modulated air flow into cell A was kept on recorder 6.

4.3 Results

Net inputs to each integrator were zeroed by trimming pots during an initial period of simulated steady-state operation. Because the controller operated on such an extremely small proportional band, steady state was marked by a continuous cycling of the control valve. The valve cycled from 30° to 37° with a period of 0.99 (real) sec.

Impulse perturbations were simulated by changing the initial condition on integrator 6, and ramp perturbations were generated by adding another constant input to integrator 6. Analog runs 1 to 14 were carried out to test the ventilation system recovery from impulse and ramp perturbations in cell A. Important results are summarized in Table 5. Run data are presented graphically in Figs. 16 through 19. The magnitude of the pressure impulse is plotted against the time lapsed before cell A returns to atmospheric pressure in Fig. 20.

The inlet damper valve was able to control the cell pressure at the design value of -1 in. H_2O for ramp perturbations up to +1 in. H_2O/sec . However, a ramp input of +2 in. H_2O/sec raised the steady-state pressure to atmospheric even though the inlet damper was fully closed. Increasing the size of the ramp perturbation further raised the steady-state pressure (Fig. 21). An input ramp of +3 in. H_2O/sec gave the response shown in Fig. 17. Return to the control point was observed by removing the disturbing function after the new steady-state pressure had been reached. Run 14 (Fig. 18) was for a ramp input of +5 in. H_2O/sec acting for a period of 6.15 sec.

Impulse perturbations of +2 in. H_2O and less did not allow the secondary containment area to reach atmospheric pressure. However, with impulses of +4 in. H_2O and greater atmospheric pressure was reached for short times. Ramp inputs greater than +1 in. H_2O/sec caused the Maintenance Facility to reach atmospheric pressure in approximately 2 sec.

One operating parameter, the valve time constant, was increased for runs 15 to 19. The first group of runs corresponded to time constants arising from 5 ft of transmission line from the controller to the valve. Larger time constants were used to simulate 28 ft of line for runs 15 to 19.

Steady-state operation was somewhat smoother with the longer transmission line. Valve cycling was decreased in both amplitude and period. For an amplitude of 31.5° to 35° , a period of 1.13 sec was observed. Run 17 (Fig. 19) showed the response to an impulse perturbation of +8 in. of water. This should be compared with the response to the same upset but with a faster acting valve (Fig. 16). The time for cell A to return to atmospheric pressure was less in run 17 because the valve was not able to close so fast, and the cell A pressure could be relieved by blowback into the Maintenance Facility.

Table 5. Results of Analog Simulation of Bldg. 3026 Ventilation System

Run No.	Length of Tubing from Controller to Valve, ft	Type of Perturbation	Magnitude of Perturbation	Maximum Maintenance Facility Pressure, in. H ₂ O	Time for Maintenance Facility to Reach Max Pressure, sec	Remarks
1	5	-	-	-	-	Steady-state
2	5	Impulse	+1 in. H ₂ O	-0.062	1.4	Cell A above atmospheric 0.36 sec
3	5	Impulse	+2 in. H ₂ O	-0.035	1.5	Cell A above atmospheric 0.65 sec
4	5	Impulse	+4 in. H ₂ O	0	0.9	Cell A above atmospheric 1.14 sec
5	5	Impulse	+6 in. H ₂ O	0	0.8	Cell A above atmospheric 1.63 sec
6	5	Impulse	+8 in. H ₂ O	0	0.8	Cell A above atmospheric 2.12 sec
7	5	Ramp	+1 in. H ₂ O/sec	-0.03	Steady-state	
8	5	Ramp	+10 in. H ₂ O/sec	0	1.3	Steady-state P ₂ off scale
9	5	Ramp	+2 in. H ₂ O/sec	0	2.4	Steady-state P ₂ = 0
10	5	Ramp	+4 in. H ₂ O/sec	0	2.0	Steady-state P ₂ = +5.5 in. H ₂ O
11	5	Ramp	+4 in. H ₂ O/sec	0	2.1	Removed ramp at P ₂ = +1 in. H ₂ O
12	5	Ramp	+4 in. H ₂ O/sec	0	1.8	Removed ramp at P ₂ = +3 in. H ₂ O
13	5	Ramp	+3 in. H ₂ O/sec	0	2.3	Steady-state P ₂ = +1.3 in. H ₂ O
14	5	Ramp	+5 in. H ₂ O/sec	0	1.7	Removed ramp at P ₂ = +8 in. H ₂ O
15	28	-	-	-	-	Steady-state
16	28	Impulse	+1 in. H ₂ O	-0.090	1.6	Cell A above atmospheric 0.34 sec
17	28	Impulse	+8 in. H ₂ O	0	0.6	Cell A above atmospheric 1.80 sec
18	28	Ramp	+2 in. H ₂ O	0	2.6	
19	28	Ramp	+4 in. H ₂ O	0	1.2	

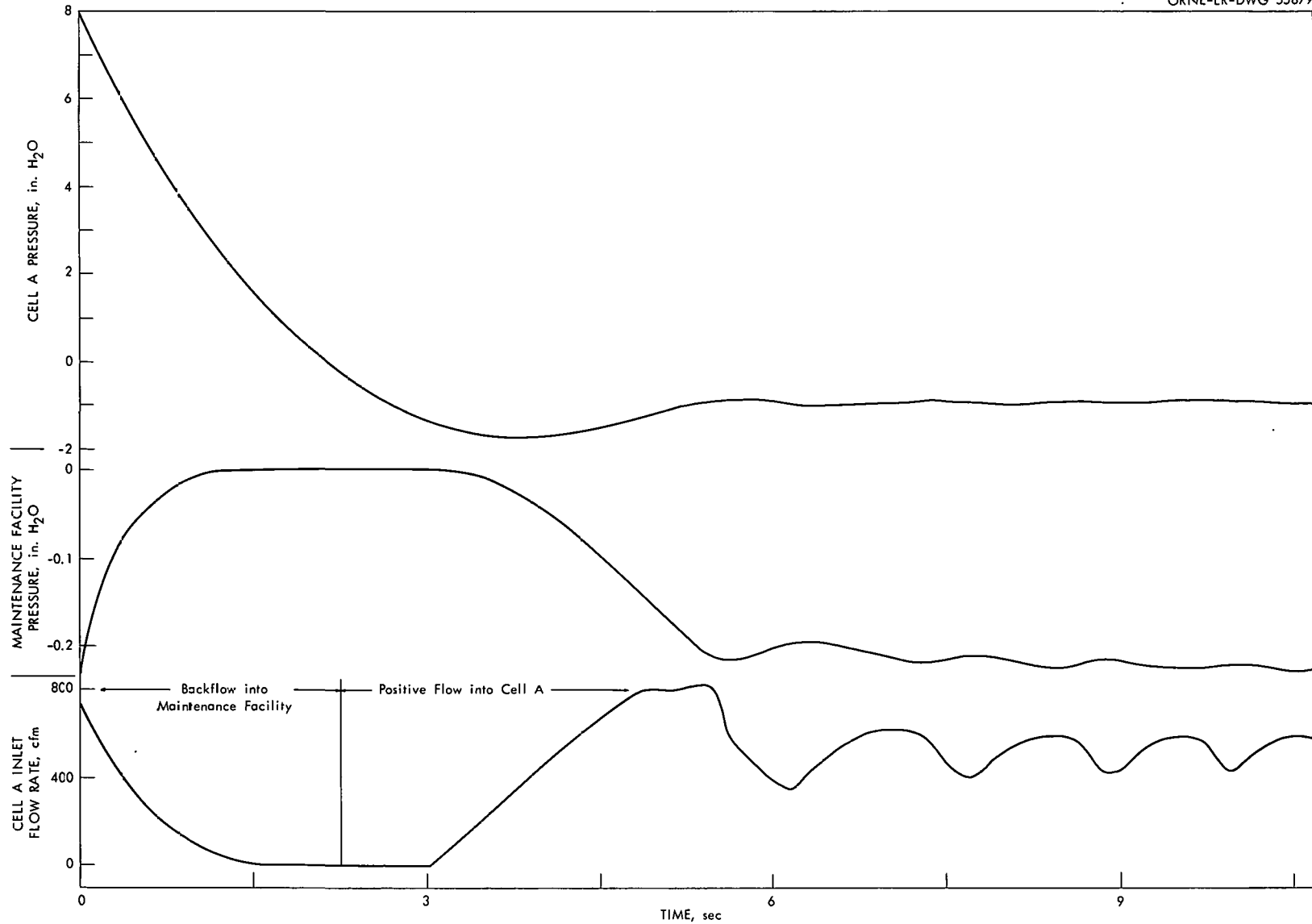


Fig. 16. Transient pressures in ventilating system of Bldg. 3026 due to an impulse perturbation in cell A of +8.0 in. H₂O; 5 ft. of tubing from controller to valve.

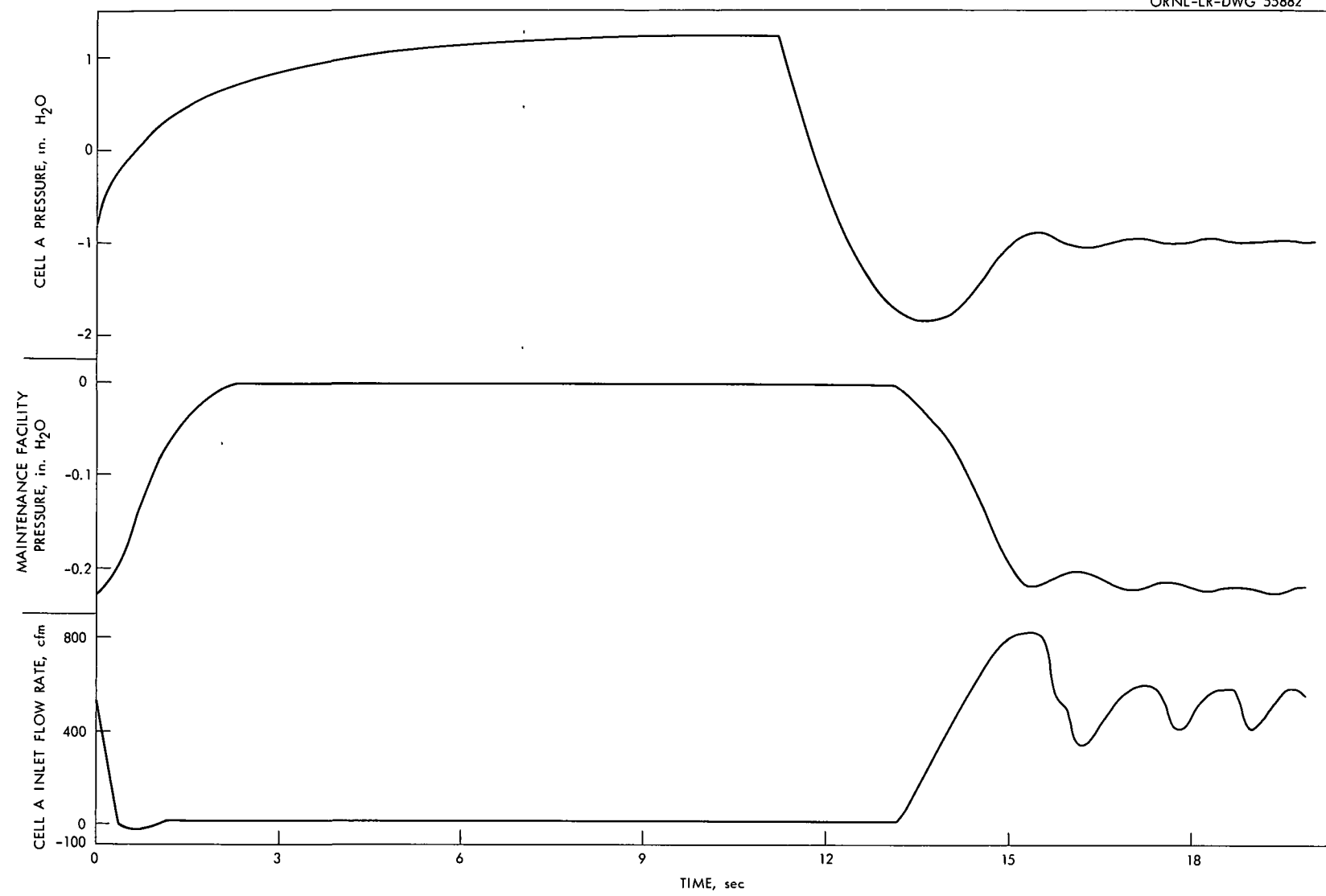


Fig. 17. Transient pressures in ventilating system of Bldg. 3026 due to a ramp perturbation in cell A of 3 in. H₂O/sec for 11.25 sec.

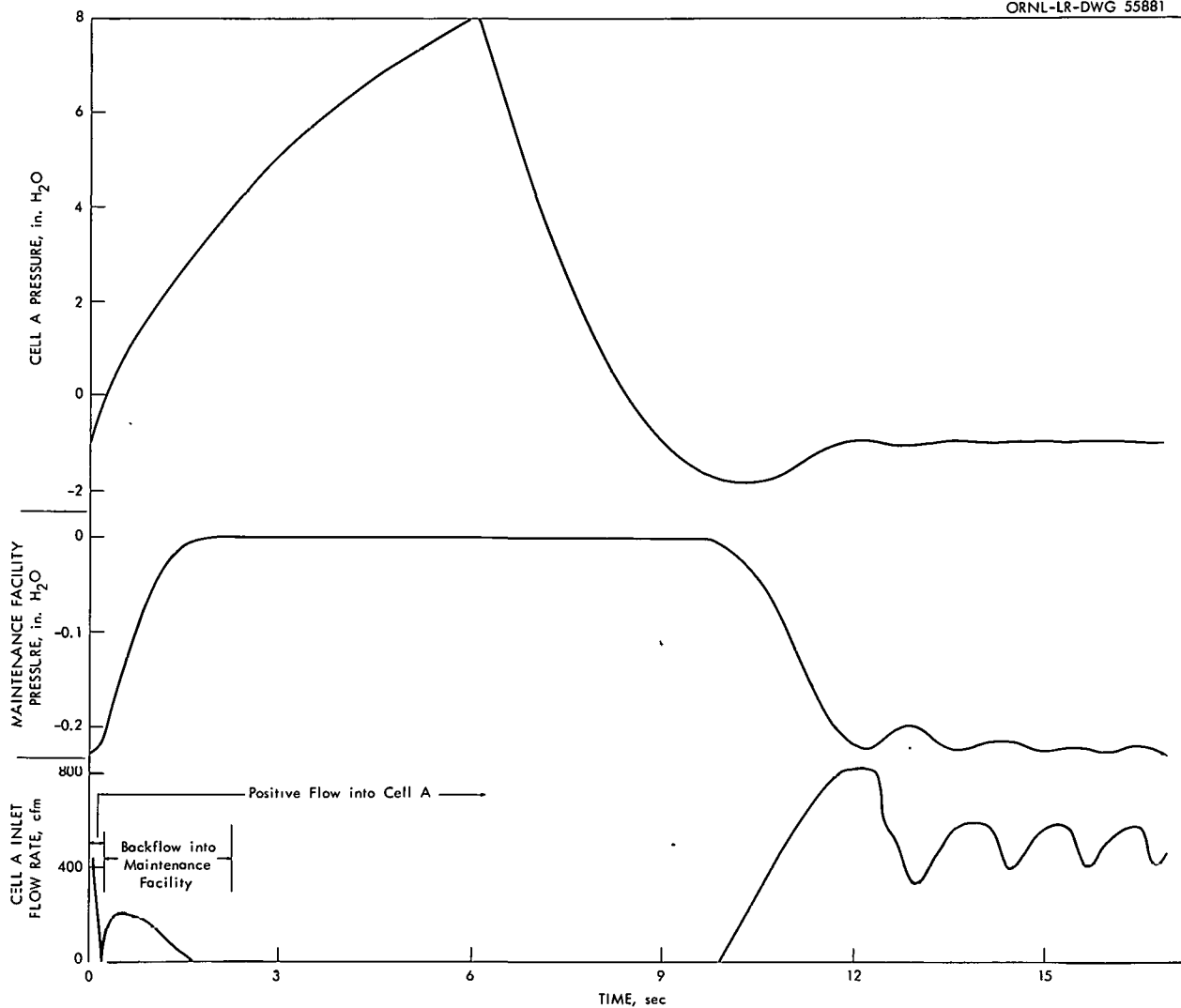


Fig. 18. Transient pressures in the ventilating system of Bldg. 3026 due to a ramp perturbation in cell A of 5 in. H₂O/sec for 6.15 sec.

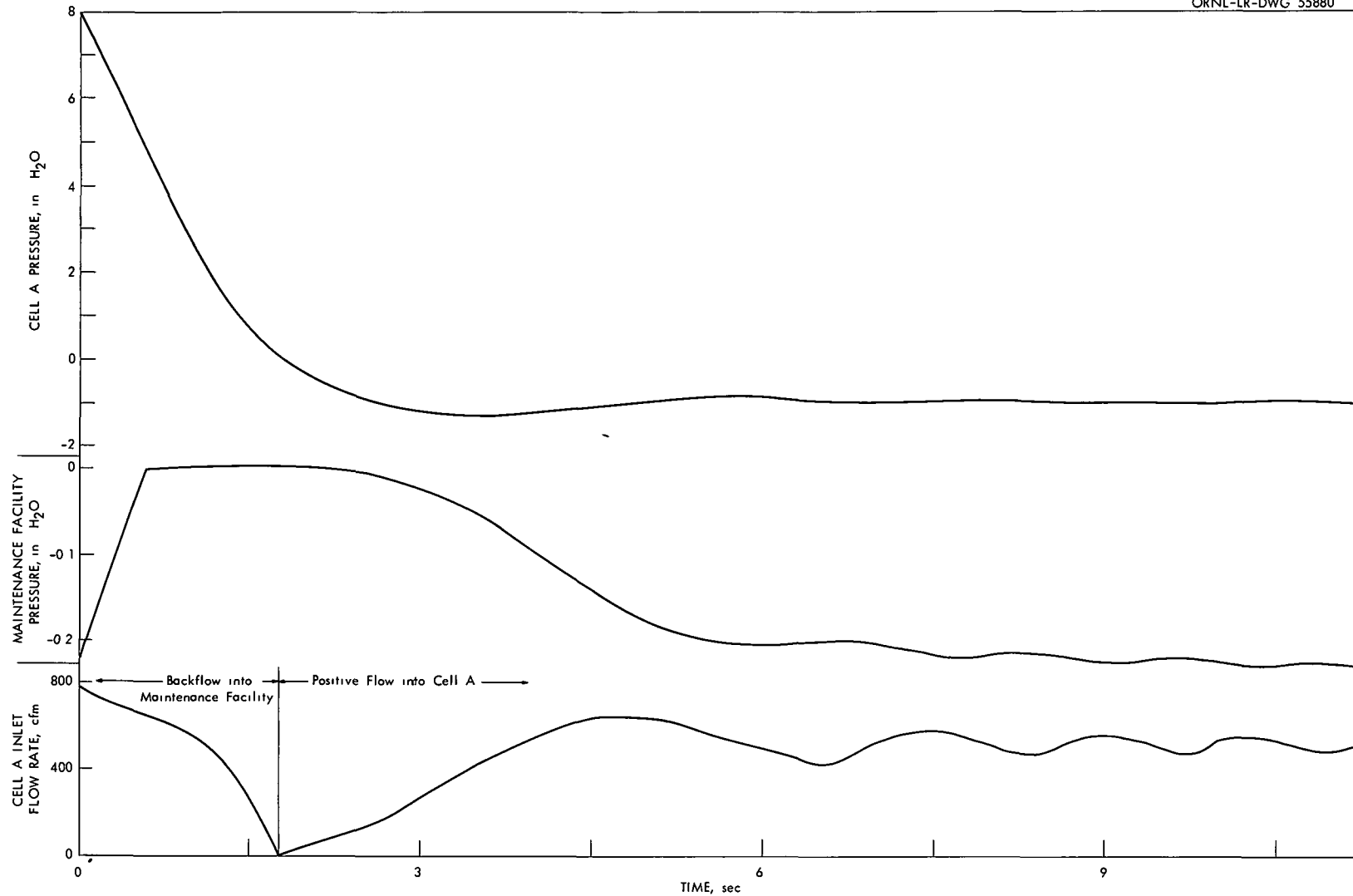


Fig. 19. Transient pressures in cell ventilating system of Bldg. 3026 due to an impulse perturbation in cell A of +8.0 in. H₂O; 28 ft. of tubing from controller to valve.

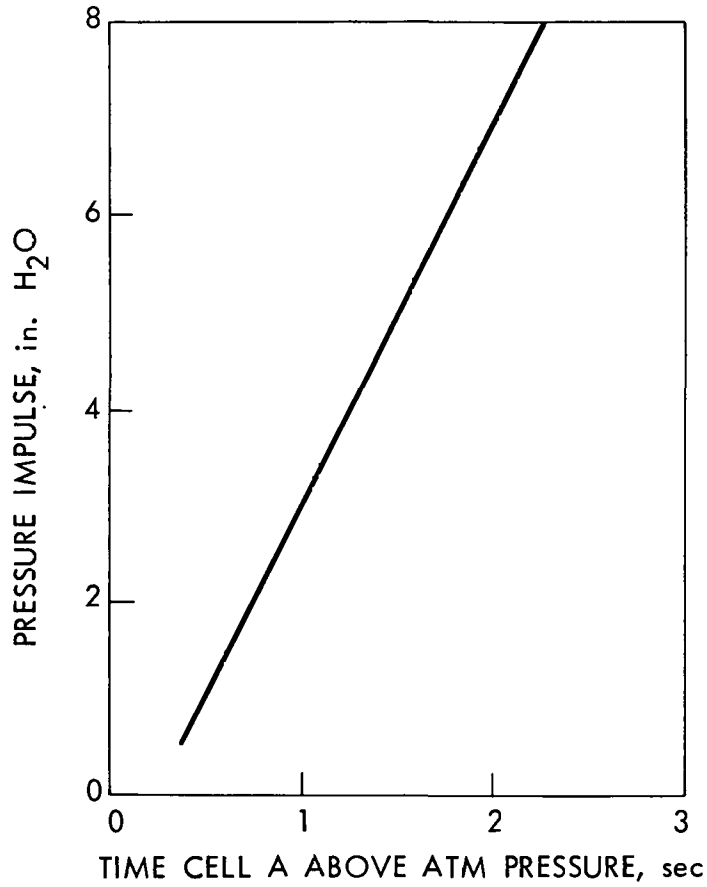


Fig. 20. Magnitude of pressure impulse vs time for cell A (Bldg. 3026) to recover to atmospheric pressure.

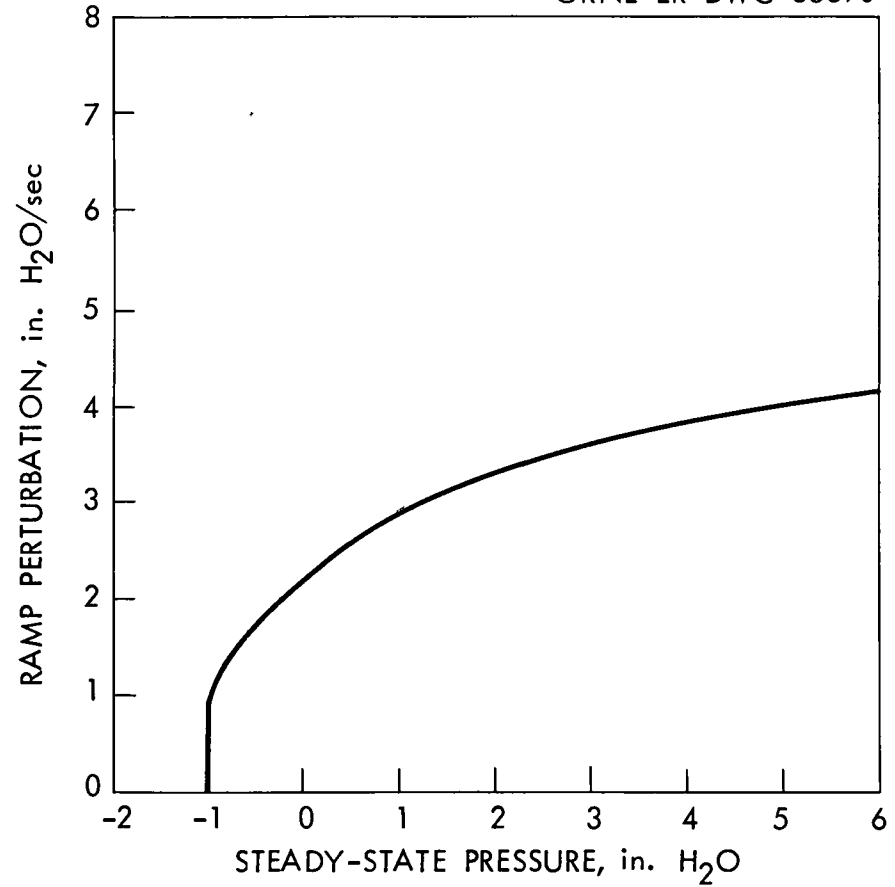


Fig. 21. Magnitude of ramp perturbation vs steady-state cell A (Bldg. 3026) pressure.

Outleakages from cell A for impulse perturbations were calculated from eq. 2-4 with $R_L = R_4 = 0.240 \text{ (in. H}_2\text{O)}^{1/2}/(\text{ft}^3/\text{sec})$. The results are shown in Fig. 22 for outleakage volumes varying from 1 ft^3 for a $1 \text{ in. H}_2\text{O}$ impulse perturbation to 11.0 ft^3 for a $6.5 \text{ in. H}_2\text{O}$ perturbation.

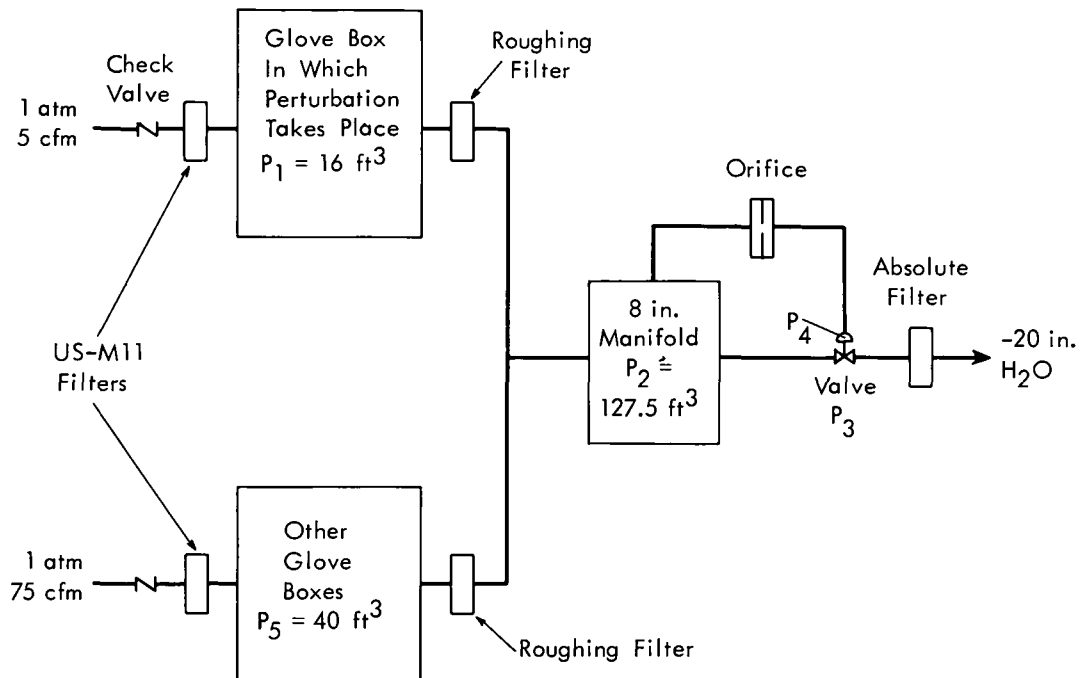
Since the leak rate of 250 used to calculate R_4 at steady state exceeds the recommended maximum of 1% of the cell volume per minute, outleakage was estimated assuming the leak rate at steady state to be 100 and 50 cfm. These results are in error because transient pressures were calculated with R_4 , but the errors are small because of the relatively low resistance of the other inlet and outlet routes. For the 50-cfm leak rate at steady state, outleakages range from 0.2 ft^3 for a $1 \text{ in. H}_2\text{O}$ impulse perturbation to 2.5 ft^3 for a $7.1 \text{ in. H}_2\text{O}$ perturbation.

5.0 CLOSED GLOVE-BOX SYSTEM IN BLDG. 3508

5.1 Description of Ventilating System

Building 3508, which was designed for work with materials emitting alpha particles, has five laboratory rooms which contain hoods and open and closed glove boxes. The hoods and open glove boxes, which are served by a local ventilating system, do not pose a problem of the type considered in this report since they operate at essentially atmospheric pressure. The closed glove boxes are vented into a common manifold, which is maintained at $-0.36 \text{ in. H}_2\text{O}$ by a control valve. The intended mode of operation of this system is to have 16 boxes on stream continuously in Lab. No. 4, with more inlets to the off-gas manifold available in Lab. No. 2 if needed. The air passes through the control valve and absolute filter and eventually to the 3039 stack.

The closed box ventilating system may be represented schematically as



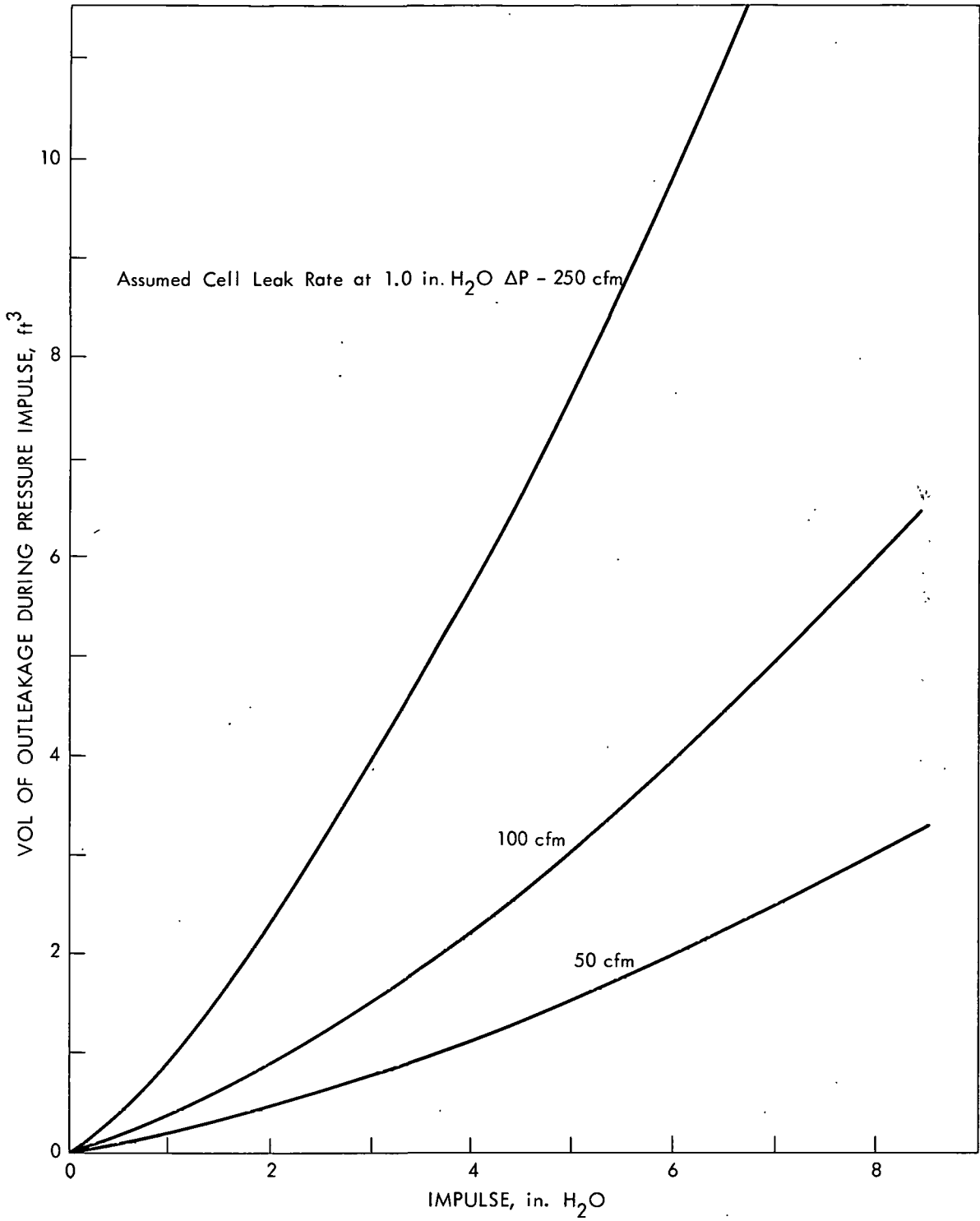


Fig. 22. Outleakage from cell A of Bldg. 3026 due to impulse perturbations.

The system was studied assuming that only the 16 boxes in Lab. No. 4 were on stream. The pressure in the manifold is controlled by a Bryant Model DSR-24 regulator. The pressure at the downstream side of the absolute filter, which may vary from -10 to -40 in. H₂O depending on the operation of the other systems served by the 3039 stack, was assumed to be constant at -20 in. H₂O. The amounts of gases that might be involved in perturbations to a 16-ft³ glove box would have a negligible effect on the pressure in this duct work, which also serves Bldgs. 3503, 3505, and 3517 and the isotope area.

5.2 Assumptions and Equations

The resistances of the filters in the ventilating system are

<u>Filter</u>	<u>Resistance,</u> <u>in. H₂O/(lb-moles/sec)</u>
Inlet to box P ₁	1633
Inlet to box P ₅	108.8
Outlet to box P ₁	173
Outlet to box P ₅	11.53
Absolute	23.3

The resistance of the regulating valve is variable, depending on the pressure in its diaphragm chamber, which is equal to the pressure in the manifold at steady state. An orifice is built into the inlet of the diaphragm chamber, presumably to damp out fluctuations in the upstream line pressure. From the results of tests on this valve, the resistance of the orifice R_O was estimated to be 32,600 (in. H₂O)^{1/2}/(lb-moles/sec). The dead volume of the diaphragm chamber, V_D (i.e., the volume of the chamber when the valve is shut), was estimated to be 0.055 ft³. Assuming a linear relation between the pressure in the chamber P₄ and the difference between the total and dead volumes of the chamber, the following equation was obtained:

$$V - V_D = 0.1572 P_4 + 0.0684 \quad 0 < V - V_D \leq 0.0212 \quad (5-1)$$

The maximum value for V - V_D (which occurs when the valve is fully open) is 0.0212 ft³. The resistance of the valve fully open is 450 (in. H₂O)^{1/2}/(lb-moles/sec). Assuming the resistance of the valve to be inversely proportional to V - V_D, the resistance of the valve was calculated to be

$$R_V = 450 \left[0.0212 / (V - V_D) \right] = 9.54 / (V - V_D) \quad (5-2)$$

To complete the analysis of the behavior of the regulator, the flow between the manifold and the diaphragm chamber must be determined. The amount of air in the chamber is

$$N_4 = P_4 V / RT \quad (5-3)$$

where N₄ = pound-moles of air in the diaphragm chamber

The rate of accumulation is given by

$$\frac{dN_4}{dt} = \frac{1}{RT} \left(V \frac{dP_4}{dt} + P_4 \frac{dV}{dt} \right) = \frac{\sqrt{P_2 - P_4}}{R_0} \quad (5-4)$$

From eq. 5-1,

$$\frac{dV}{dt} = 0.1572 \frac{dP_4}{dt} \quad (5-5)$$

$$\frac{dN_4}{dt} = \left(\frac{V - V_D + V_D}{RT} \right) \frac{dP_4}{dt} + \frac{P_4 (0.1572)}{RT} \frac{dP_4}{dt} \quad (5-6)$$

$$\frac{dN_4}{dt} = \left(\frac{0.3144 P_4 + 0.1233}{RT} \right) \frac{dP_4}{dt} = \frac{\sqrt{P_2 - P_4}}{R_0} \quad (5-7)$$

The equations describing the behavior of the ventilating system with eq. 5-1 may be set down as follows:

$$\frac{dP_1}{dt} = 5.99(-P_1) - 56.5(P_1 - P_2) \quad (5-8)$$

$$\frac{dP_5}{dt} = 5.99(-P_5) - 56.5(P_5 - P_2) \quad (5-9)$$

$$\frac{dP_2}{dt} = 7.09(P_1 - P_2) + 106.3(P_5 - P_2) - 128.4(V - V_D) \sqrt{P_2 - P_3} \quad (5-10)$$

$$(V - V_D) \sqrt{P_2 - P_3} = 0.409(P_3 + 20) \quad (5-11)$$

$$(0.314 P_4 + 0.1233) \frac{dP_4}{dt} = 4.80 \sqrt{P_2 - P_4} \quad (5-12)$$

In the derivation of eq. 5-11 it was assumed that the capacitance associated with P_3 was negligible. Where the quantity $V - V_D$ occurs explicitly in eqs. 5-1 and 5-8 through 5-11, its value was limited between 0 and 0.0212 ft³ by analog computer circuitry (Sect. 5.3). However, this limitation was not taken into account in the application of eq. 5-12, in which the limitation occurs implicitly. Therefore there is some error in the length of time before the valve closes following the cutoff of a perturbation, but the error occurs only after the results of interest have been obtained.

The steady-state pressures in the ventilating system are

$$P_1 = -0.350 \text{ in. H}_2\text{O}$$

$$P_2 = -0.387$$

$$P_3 = -19.387$$

$$P_4 = -0.387$$

$$P_5 = -0.350$$

5.3 Analog Computer Circuitry

A block diagram of the analog computer circuitry for the solution of eq. 5-1 and eqs. 5-8 through 5-12 is given in Fig. 23. The switching circuit associated with amplifier 20 was used to limit $V - V_D$ to a maximum of 0.0212 volt, thereby limiting the resistance of the regulator to a minimum corresponding to the fully open position. With the potentiometer settings listed, 100 sec of machine time represents 1 sec of problem time.

5.4 Results

An example of the effects of an impulse perturbation is shown in Fig. 24, where P_1 rises instantly to +18.8 in. H_2O and requires 0.152 sec to drop back below atmospheric pressure. P_2 rises to a maximum of +0.32 in. H_2O in 0.03 sec and P_5 to a maximum of +0.17 in. H_2O in 0.055 sec. P_4 rises slightly higher than atmospheric pressure. The regulator valve position, as shown by $V - V_D$, remained at the fully open position for 0.26 sec. The valve then dropped to fully closed as P_2 dropped down below its steady-state value to a minimum of -0.45 in. H_2O , before rising to approach the steady-state value. The overshoot of P_2 and P_5 of their steady-state values was caused by the orifice in the line between the manifold and the diaphragm chamber of the valve, which restricted the flow of air and delayed the response of the valve.

Examples of the effects of ramp perturbations are shown in Figs. 25 and 26. With a ramp perturbation of 200 in./sec for 0.34 sec, P_1 rose to +4.6 in. H_2O and then required 0.33 sec to drop below atmospheric pressure. P_2 and P_5 rose to maximums of 1.2 and 1.0 in. H_2O . The secondary peak in P_4 was caused by momentary instability of the servomultiplier 3-X being driven by amplifier 22 as the voltage input to 3-X passed through zero. The overshoot of P_2 and P_4 was quite spectacular for this case, with P_2 reading a minimum of -0.9 in. H_2O and P_4 reaching -0.82 in. H_2O . From eq. 5-12 it may be seen that dP_4/dt approaches infinity as P_4 approaches -0.390 in. H_2O , which corresponds to a value of $V - V_D$ approaching zero. This relation is shown in Fig. 25 by the vertical slope of P_4 during part of the overshoot period. All points had returned to their steady-state pressures 1.3 sec after the start of the perturbation. With a ramp perturbation of 1000 in. H_2O /sec for 0.021 sec, P_1 rose to +12.4 in. H_2O and then required 0.164 sec to drop below atmospheric pressure. P_2 and P_5 rose to maxima of +0.4 and +0.28 in. H_2O .

A plot of the time required for a glove box in 3508 to drop below atmospheric pressure following impulse perturbations up to 20 in. H_2O is shown in Fig. 27. The minimum impulse perturbation which causes P_2 to exceed atmospheric pressure is +10 in. H_2O .

The results of the ramp perturbation calculations are given in Table 6. Perturbation intensities from 10 to 1000 in. H_2O /sec were studied. New steady-state values for P_1 with perturbations of 10 and 100 in. H_2O /sec are -0.20 and +3.10 in. H_2O . Ramp perturbations of 200 in. H_2O /sec can be tolerated for several tenths of a second, while perturbations of 1000 in. H_2O /sec can be tolerated for only a few hundredths of a second.

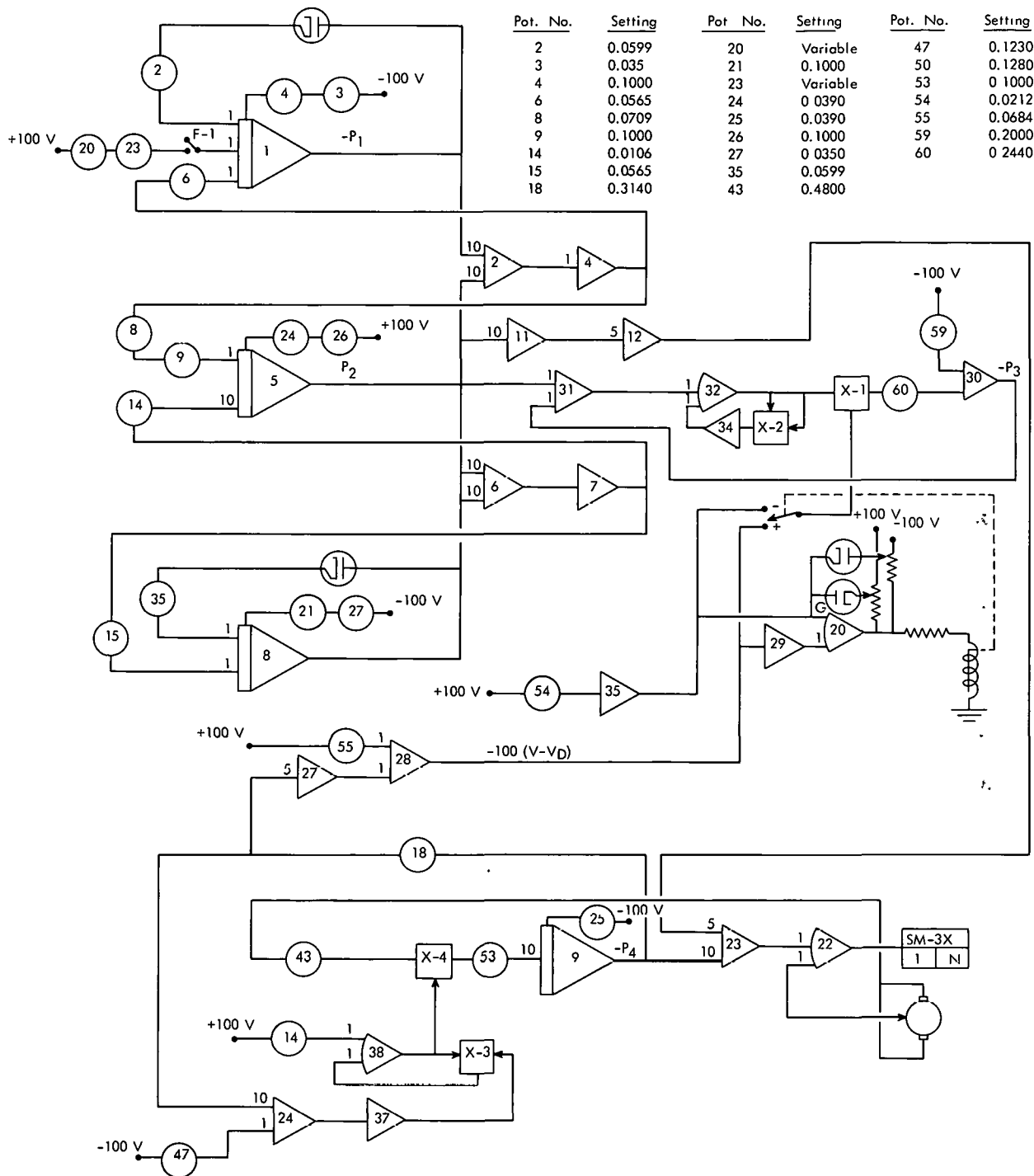


Fig. 23. Analog computer block diagram for calculating transient pressures in glove box ventilating system in Bldg. 3508.

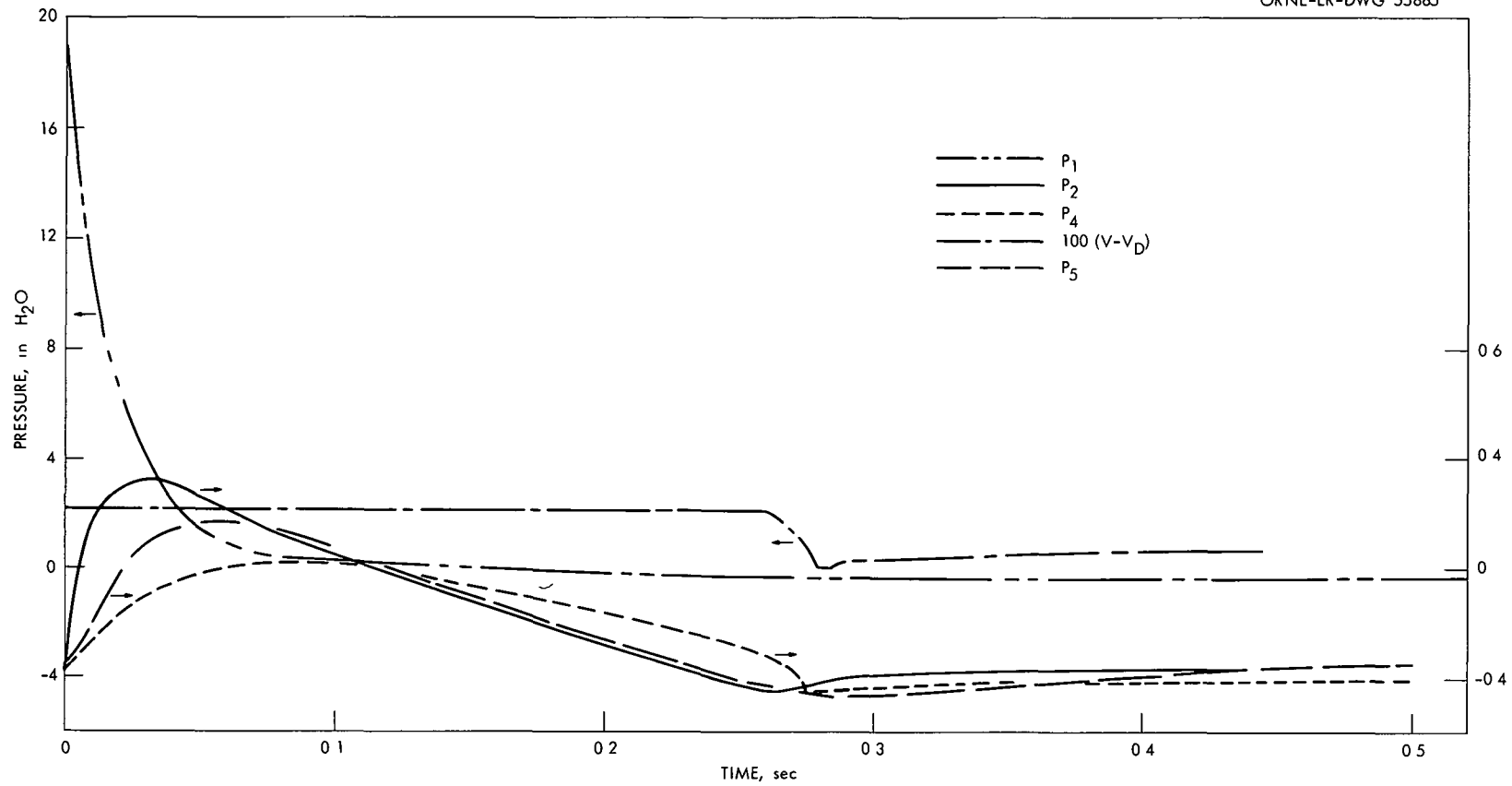


Fig. 24. Transient pressures in closed glove box ventilating system of Bldg. 3508 due to an impulse perturbation of +18.8 in. H₂O.

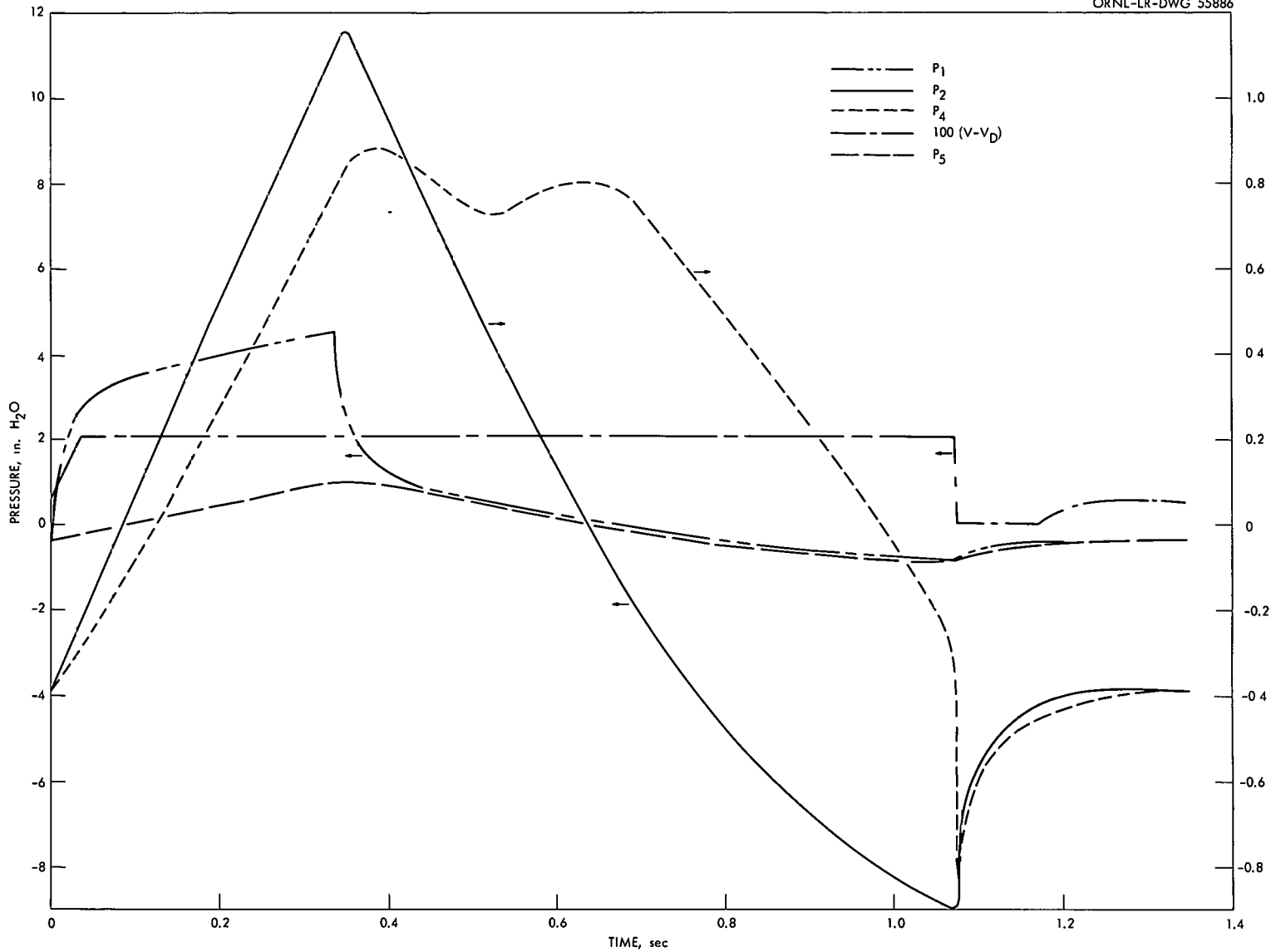


Fig. 25. Transient pressures in closed glove box ventilating system of Bldg. 3508 due to a ramp perturbation of 200 in. H₂O/sec.

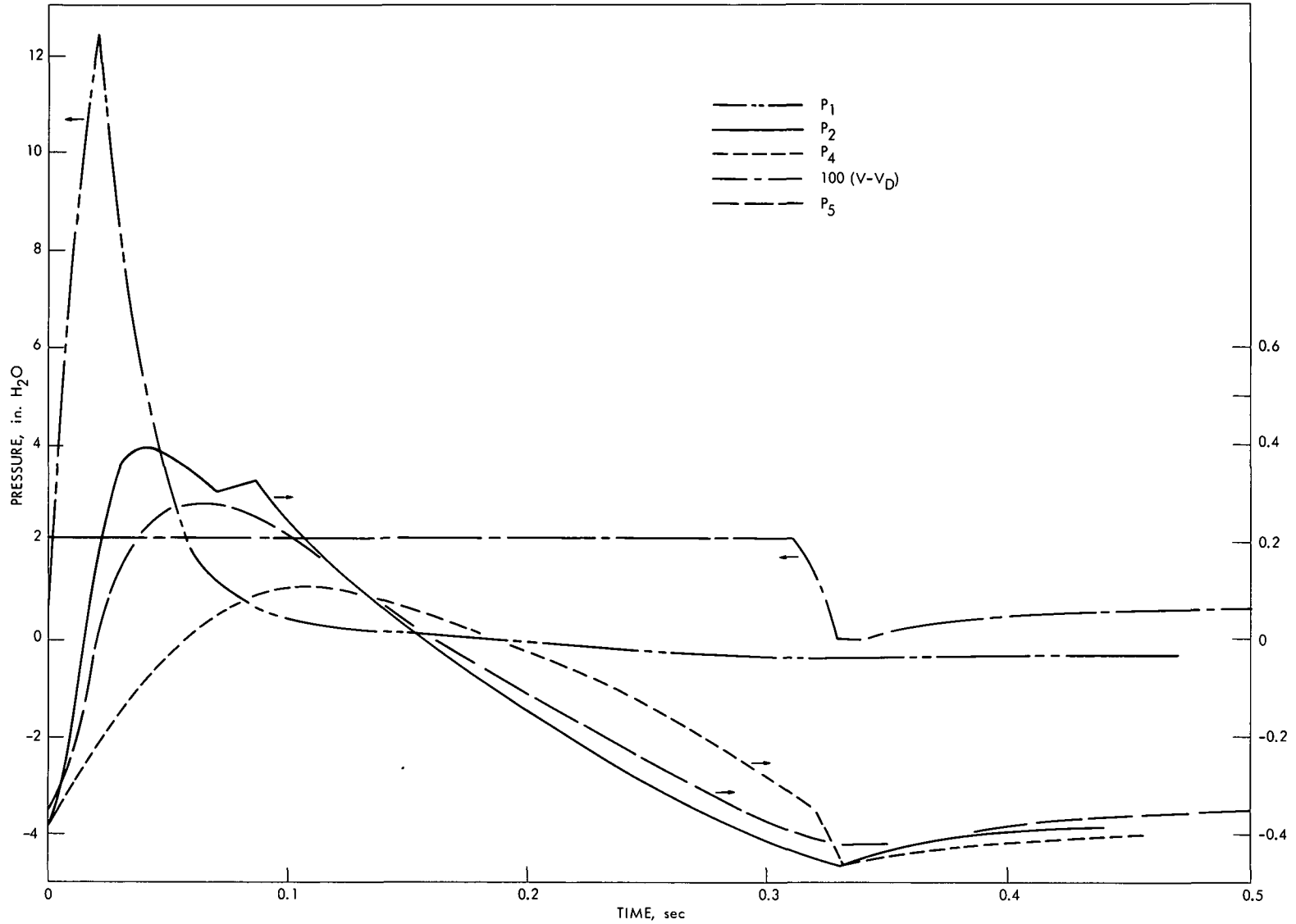


Fig. 26. Transient pressures in closed glove box ventilating system of Bldg. 3508 due to a ramp perturbation of 1000 in. H₂O/sec.

UNCLASSIFIED
ORNL-LR-DWG. 59770

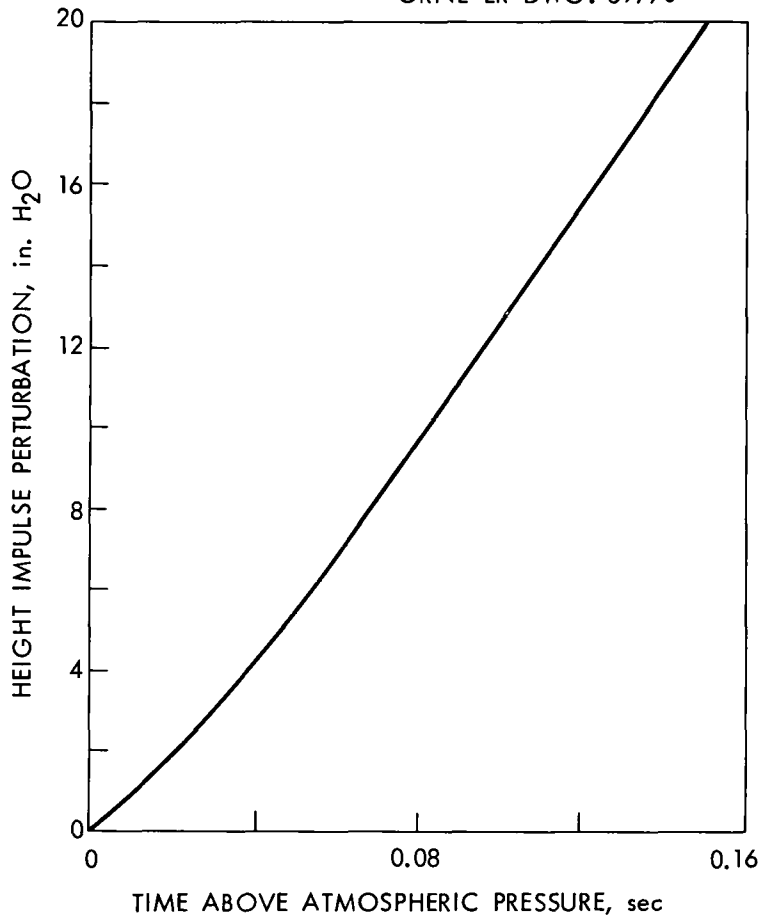


Fig. 27. Time required for glove box in Bldg. 3508 to drop below atmospheric pressure after an impulse perturbation.

The outleakage was calculated from eq. 2-4, using the permissible inleakage rate of 1% of the glove box volume per minute under normal conditions to calculate a value for R_L . The leakage rate should not exceed 0.16 ft³/min at -0.35 in. H₂O, giving a value for R_L of 3.70 (in. H₂O)^{1/2}/(ft³/min). Applying eq. 2-4 to the data in Figs. 24 through 26, the outleakages were calculated to be 0.092 ft³ for the impulse perturbation of +18.8 in. H₂O, and 3.97 and 0.12 ft³ for the ramp perturbations of 200 in. H₂O/sec for 0.34 sec and 1000 in. H₂O/sec for 0.021 sec.

6.0 CELL VENTILATION SYSTEM IN BLDG. 4507

6.1 Description of Ventilation System

Building 4507 is used for radiochemical separation process studies with highly irradiated fuel. Small sections of irradiated fuel, prototype fuel elements, or irradiated fuel pins containing relatively small amounts of fission products and heavy elements are dissolved for laboratory-scale process development. Cells housing one cycle of solvent extraction, a

Table 6. Effects of Ramp Perturbations of Closed Glove-box Ventilating System in Bldg. 3508

Intensity, in. H ₂ O/sec	Length, sec	Max P ₁ , in. H ₂ O	Max P ₂ , in. H ₂ O	Total Time P ₁ above Atmospheric Pressure, sec
10	∞	-0.20	-0.37	0
100	11.02	+3.10	+1.44	11.39
200	0.34	+4.55	+1.13	0.67
200	0.21	+4.00	+0.61	0.40
200	0.05	+3.00	-0.13	0.10
350	0.15	+7.00	+1.17	0.47
350	0.06	+6.00	+0.29	0.19
350	0.03	+4.90	-0.02	0.10
500	0.07	+8.90	+0.71	0.29
500	0.03	+6.90	+0.10	0.11
500	0.02	+5.60	-0.06	0.08
1000	0.03	+14.40	+0.72	0.25
1000	0.02	+12.40	+0.40	0.18
1000	0.01	+10.2	+0.22	0.12

complete fused-salt fluoride-volatility plant, and two general-purpose cells for dissolution and high-level waste disposal must contain the radioactive materials processed. In various processing stages, fission products may be expected to be present as solutions, solids, or gases. In addition, volatile compounds of heavy elements will be present. Very high activity level experiments will be done in the future.

Secondary containment is provided by the entire building surrounding the main cell block. Figures 28 through 30 show the overall ventilation flow schemes of the secondary and primary containment areas.

Fans in the change room and the penthouse discharge building air to the atmosphere through absolute filters. Building pressure will normally be controlled to approximately -0.1 in. H₂O with respect to the atmosphere by means of automatic dampers on inlets and on the penthouse fan discharge.

Neglecting building inleakage, all air makeup must pass through dust stop filters through one of four openings: two in the operating area, one at the air conditioner, and one in the penthouse.

If the building air should become contaminated, as indicated by air radiation monitors, all air inlets to the building can be closed and the fans stopped, either automatically or by manually operated switches. The building will then be exhausted to -0.3 in. H₂O via a normally closed duct from the penthouse to the cell exhaust header. The cell ventilation system



UNCLASSIFIED
ORNL-LR-DWG 47939 R1

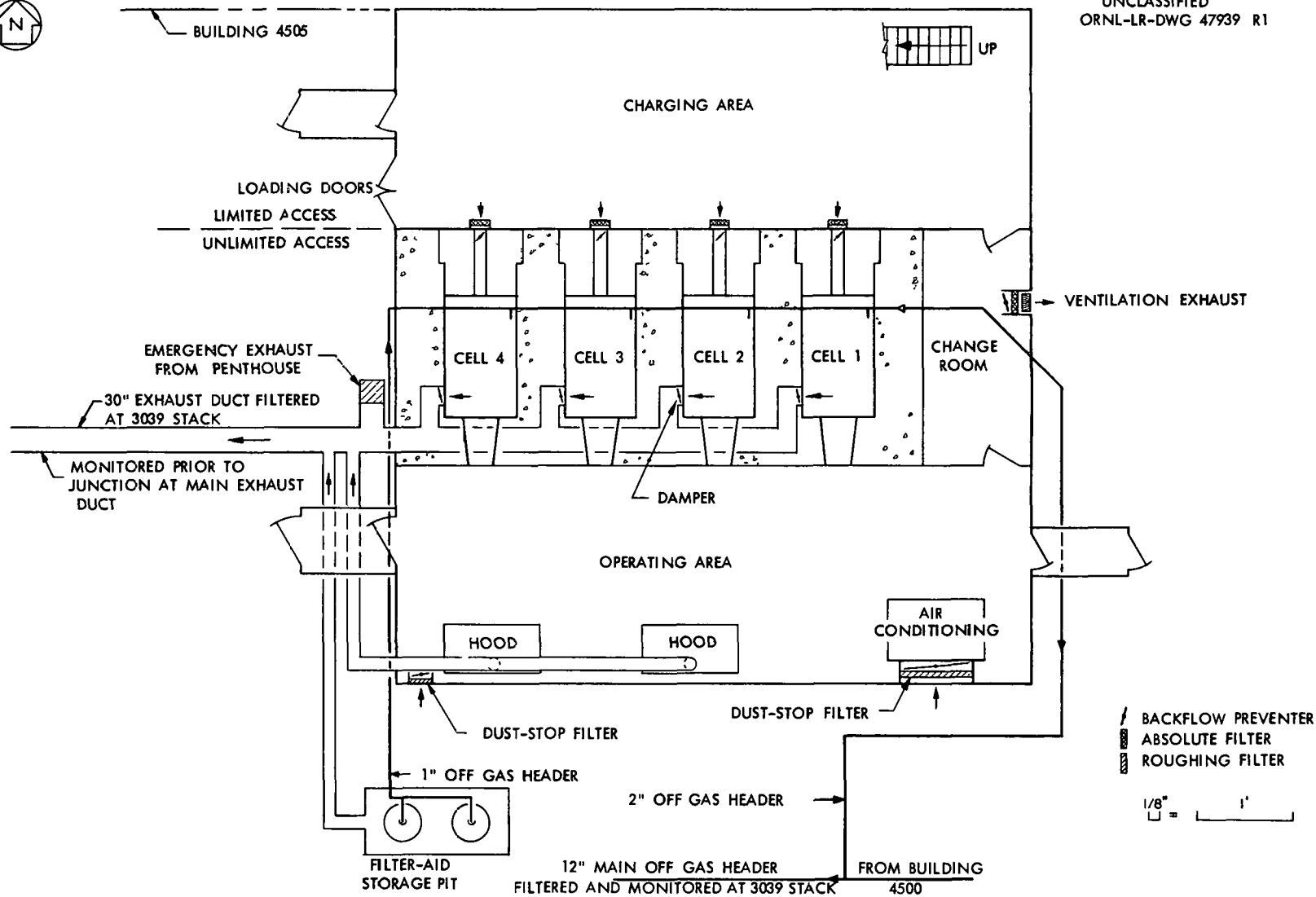


Fig. 28. Building 4507 first floor plan ventilation schematic.

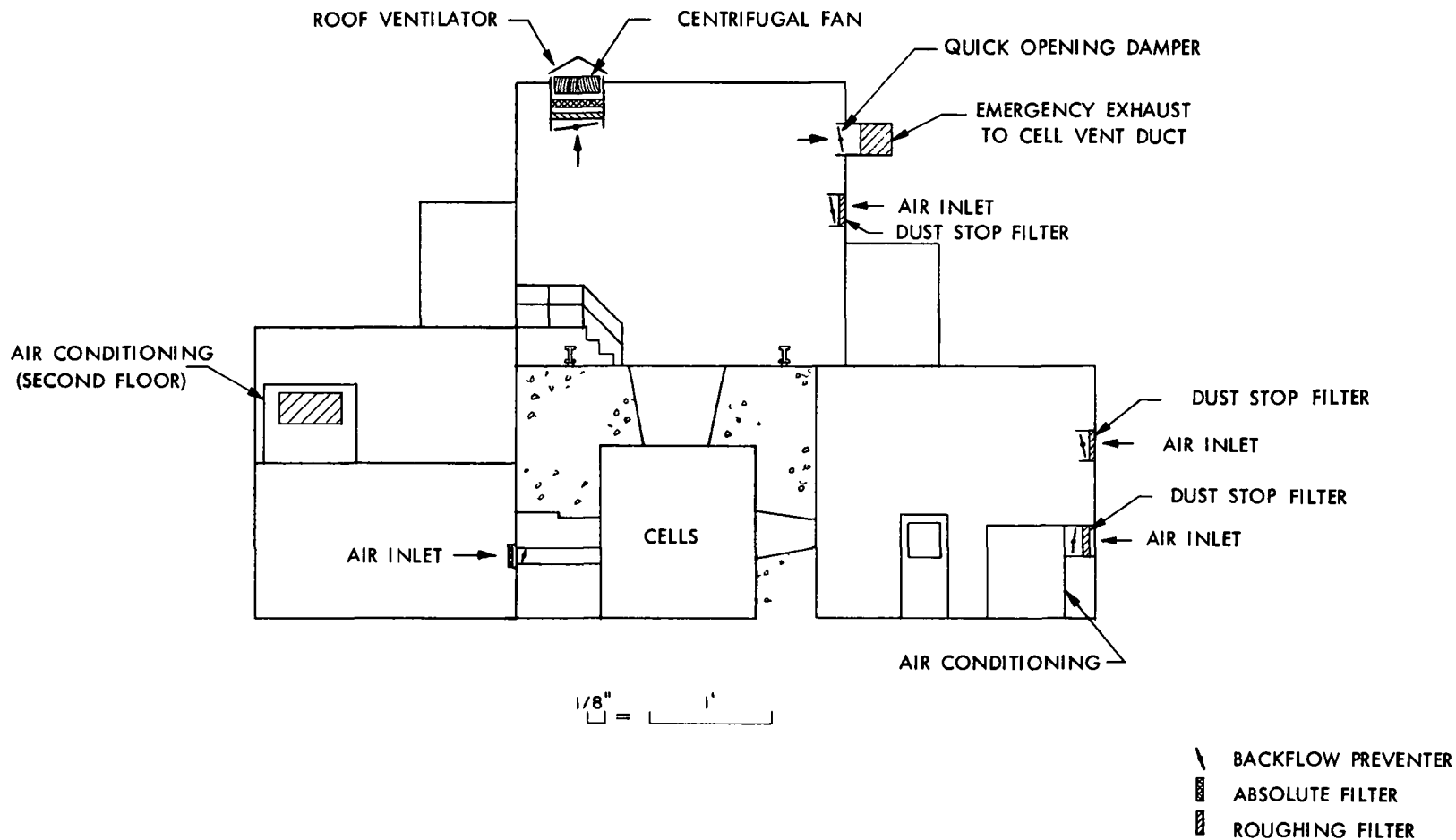
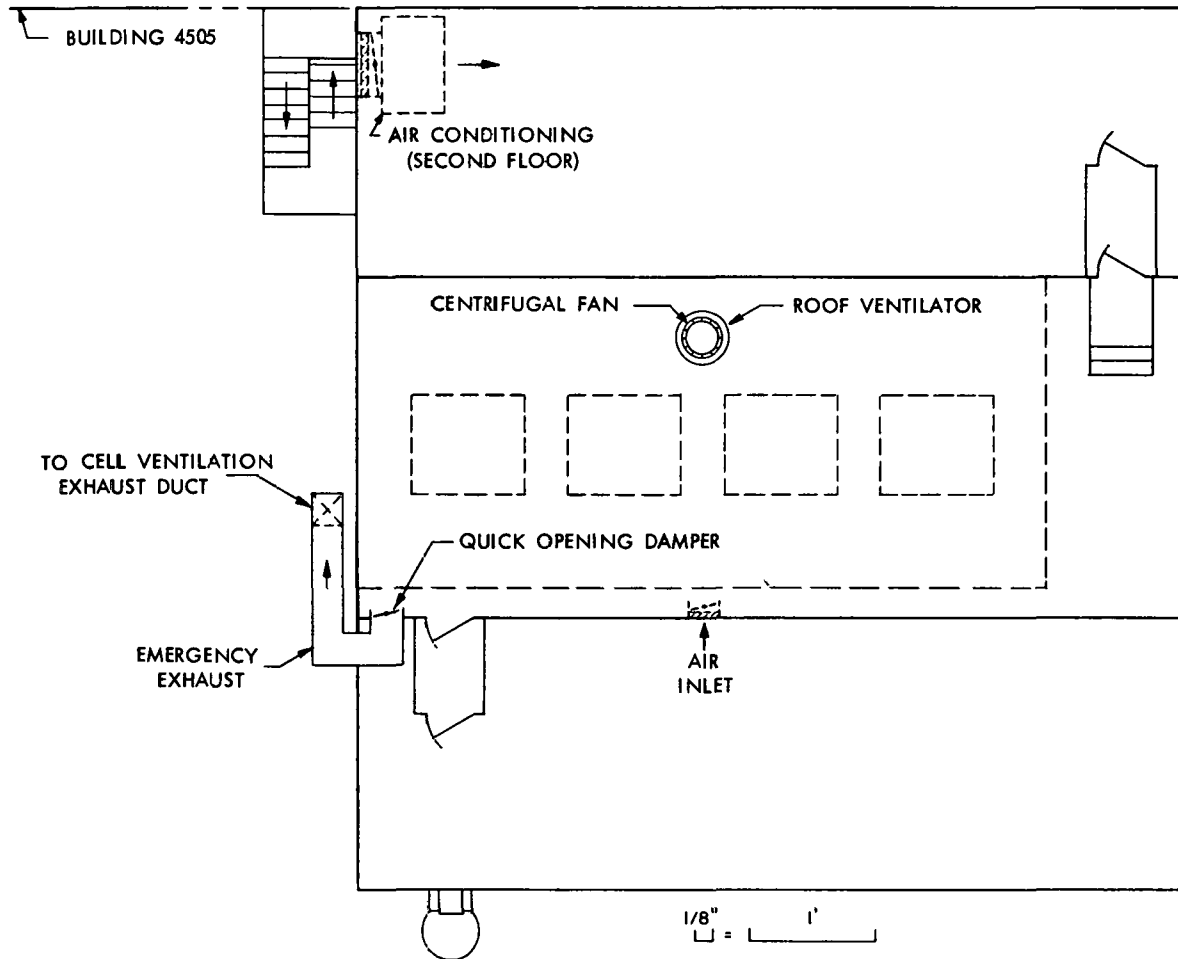


Fig. 29. Building 4507 section view ventilation schematic.



-55-



-  BACKFLOW PREVENTER
-  DUST-STOP FILTER

Fig. 30. Building 4507 roof plan ventilation schematic.

removes air from each cell through a 16- by 24-in. vent at the cell base which connects to a 30-in. header leading to the 3039 stack. A single blower at the stack services cell ventilation from Bldgs. 4500, 4501, 4505, and 4507. The capacitance of the duct is large, and the increased flow resulting from a pressure surge in one of the Bldg. 4507 cells would be very small compared to the total flow to the stack. In the analysis to follow, this duct was treated as an infinite sink at a constant pressure of -8 in. H₂O.

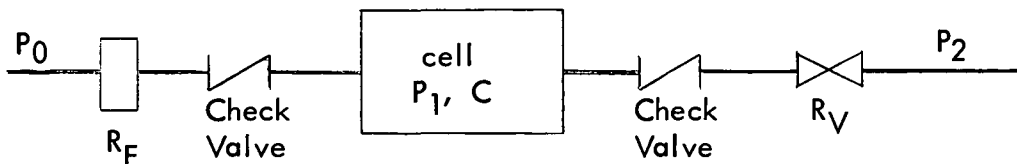
Manually operated damper valves and possibly backflow preventers will be installed in the vent lines from each cell.

Air flow enters each of the four shielded cells in Bldg. 4507 from the charging area through ductwork fitted with two sets of one absolute filter preceded by a roughing filter connected in parallel. Backflow preventers were also incorporated into the entrance ducts so that there would be no backflow into the secondary containment area via the entrance duct. Even if the backflow preventer failed open, the filter combinations would serve as a secondary line of defense to contain any activity during pressure transients.

No controller action has been designed for the cell ventilation system. Rather, the cell pressure will be continuously monitored with alarm type instruments to ensure that a pressure drop of -1.0 in. H₂O is maintained between the operating area and each cell. The manual damper valve on the cell exhaust line provides a means of regulating the cell pressure. Since there is no damper planned for throttling the inlet air, an air flow rate of 1980 cfm into each cell will be realized to meet the -1.0 in. H₂O relative pressure requirement.

6.2 Mathematical Model

A simplified flow pattern diagram of a typical cell broken down to pure resistances and capacitances may be represented as



The nomenclature and numerical values are:

Filter resistance	R_F	5.05×10^{-4} in. H ₂ O/cfm
Damper valve resistance	R_V	1.33×10^{-3} (in. H ₂ O) ^{1/2} /cfm
Cell capacitance (free volume)	C	594 ft ³
Cell inlet flow rate	q_1	1980 cfm
Cell exit flow rate	q_2	1980 cfm
Secondary containment pressure	P_0	-0.1 in. H ₂ O
Cell pressure	P_1	-1.1 in. H ₂ O
Exhaust header pressure	P_2	-8 in. H ₂ O

For purposes of analysis, it will be assumed that the secondary containment area pressure remains constant during a pressure perturbation. This actually assumes two factors: (1) If a pressure upset occurred, no activity would be released so that an emergency evacuation to -0.3 in. H₂O would not be realized; (2) sudden loss of flow through one of the cells would not affect the secondary containment area pressure because of the very large building volume and the facts that flow through the other cells will still be maintained and the secondary containment pressure is controlled. Even if this assumption did not actually describe the real situation, the pressure range in this area is only from -0.1 in. H₂O to atmospheric, and this pressure has relatively little effect on the cell pressure.

6.3 Transient Response to Step Change in Cell Pressure

The recovery of cell pressure from an impulse pressure input may be determined by considering the air material balance equation about the cell in which the perturbation occurs.

For impulses of cell pressure to greater than -0.1 in. H₂O, the back-flow preventer will close, and the following balance applies until the cell returns to -0.1 in. H₂O:

$$\frac{C}{RT} \frac{dP_1}{dt} = - \frac{\sqrt{P_1 - P_2}}{R_V} \quad (6-1)$$

Equation 6-1 is integrated to

$$\int \frac{dP_1}{\sqrt{P_1 - P_2}} = - \frac{RT}{CR_V} \int dt \quad (6-2)$$

so that

$$2(P_1 - P_2)^{1/2} = - \frac{RT}{CR_V} t + K \quad (6-3)$$

with K = integration constant

C = cell volume

Return to the steady-state value of -1.1 in. H₂O from -0.1 in. H₂O may be followed by rewriting the material balance equation to take into account the flow through the now operated backflow preventer:

$$\frac{dP_1}{dt} = \frac{RT}{C} \left(\frac{P_0 - P_1}{R_F} - \frac{\sqrt{P_1 - P_2}}{R_V} \right) \quad (6-4)$$

Equation 6-4 was solved numerically by finite difference techniques. The results of this solution combined with the solution to eq. 6-3 yield the overall response to a step change in pressure. These are presented graphically in Fig. 31 for impulses of +5, +10, and +15 in. H₂O. Figure 32 illustrates how increasing pressure impulses result in larger times for the cell to recover to atmospheric pressure.

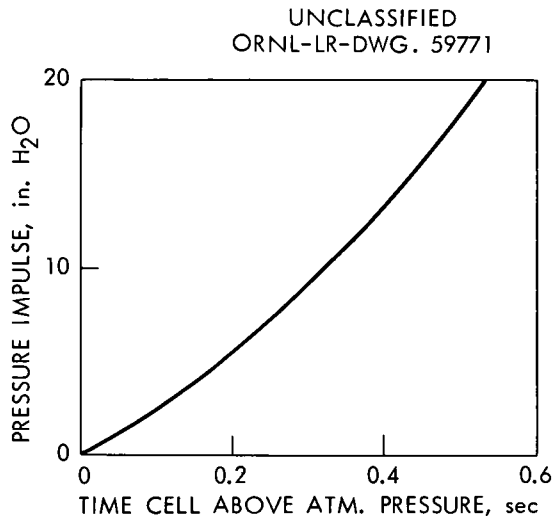


Fig. 31. Magnitude of impulse perturbation vs time for cell to recover to atmospheric pressure Bldg. 4507.

Recovery times are very short; for example, an initial pressure impulse of +18 in. H₂O will be dissipated to atmospheric pressure in only 0.5 sec (Fig. 31). Qualitatively the fast responses may be attributed to both the relatively small cell volumes and the small resistance in the damper valve on the exit vent.

6.4 Transient Response to Ramp Perturbations

The material balance from an additional input of Q cfm into a cell becomes

$$\frac{dP_1}{dt} = \frac{RT}{C} \left(Q + \frac{P_0 - P_1}{R_F} - \frac{\sqrt{P_1 - P_2}}{R_V} \right) \quad (6-5)$$

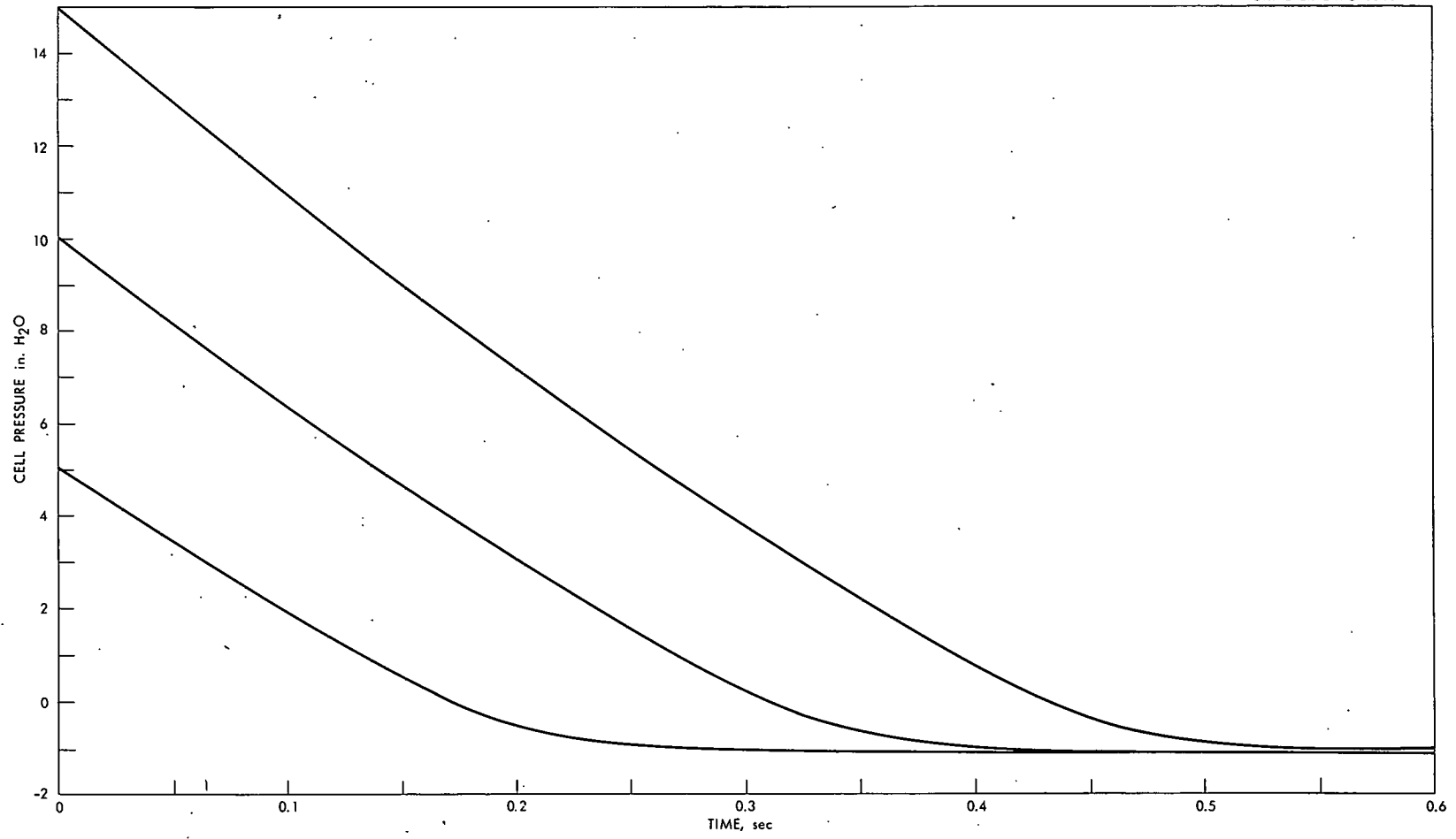


Fig. 32. Cell pressure response to impulse perturbations of +5, +10, and +15 in. H₂O Bldg. 4507.

Equation 6-5 applies only when the cell pressure is less than -0.1 in. H₂O and the backflow preventer is open. If the ramp input is large enough to ultimately raise the cell pressure to above -0.1 in. H₂O, the backflow preventer closes and the second term on the right-hand side of eq. 6-5 drops out:

$$\frac{dP_1}{dt} = \frac{RT}{C} \left(Q - \frac{\sqrt{P_1 - P_2}}{R_V} \right) \quad (6-6)$$

The steady-state cell pressure resulting from a ramp input may be calculated from eq. 6-5 for $P_1 < -0.1$ or eq. 6-6 for $P_1 > -0.1$ with $dP_1/dt = 0$. The results of these solutions are shown in Fig. 33. Ramp inputs from 0 up to 27 in. H₂O/sec raise the steady-state pressure from the design value of -1.1 in. to -0.1 in. H₂O. There is a sharp break in the curve at the -0.1 in. H₂O point because the backflow preventer closes, and the steady-state pressure increases more rapidly with increasing ramp upsets.

Equation 6-5 was solved numerically for several values of ramp perturbations. Calculations were terminated if and when the cell pressure reached -0.1 in. H₂O, and an analytical solution to eq. 6-6 was developed to follow the pressure-time curve with the backflow preventer closed.

Redefining constants and variables in eq. 6-6, let

$$a = QRT/C \text{ (constant)} \quad (6-7)$$

$$b = RT/CR_V \text{ (constant)} \quad (6-8)$$

$$u = b\sqrt{P_1 + 8} \text{ (new variable)} \quad (6-9)$$

So that

$$u^2 = b^2 (P_1 + 8) \quad (6-10)$$

Then

$$2u \, du = b^2 dP_1 \quad (6-11)$$

Substituting into eq. 6-6:

$$\frac{2}{b^2} \int \frac{u \, du}{a - u} = \int dt \quad (6-12)$$

Integrating:

$$\frac{2}{b^2} [-u - a \ln (a - u)] = t + K' \quad (6-13)$$

where K' = integration constant

UNCLASSIFIED
ORNL-LR-DWG. 59772

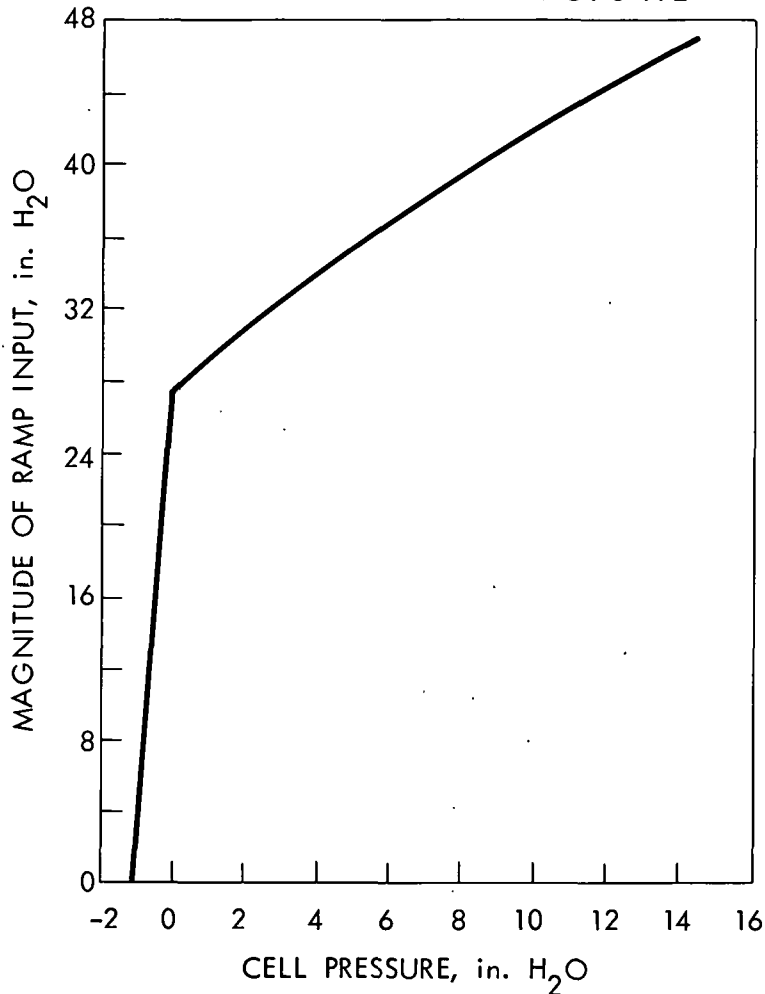


Fig. 33. Magnitude of ramp input vs steady-state cell pressure Bldg. 4507.

Integration constants were calculated by specifying the initial conditions of P and t in eq. 6-13 as the final conditions of the numerical solution.

The combined results of the numerical solution to eq. 6-5 with the analytical solution to eq. 6-6 are shown in the form of pressure-time plots in Fig. 34 for ramps of 16.4, 27.5, 32.5, and 45.5 in. of H₂O/sec.

Outleakages from a cell for impulse perturbations were calculated from eq. 2-4 with R_L taken as $0.105 (\text{in. H}_2\text{O})^{1/2}/(\text{ft}^3/\text{sec})$, obtained from a leakage rate of 5.94 cfm at a ΔP of 1.1 in. H₂O. Outleakages varied from 0.02 ft³ for an impulse perturbation of 5 in. H₂O to 0.09 ft³ for a perturbation of 15 in. H₂O.

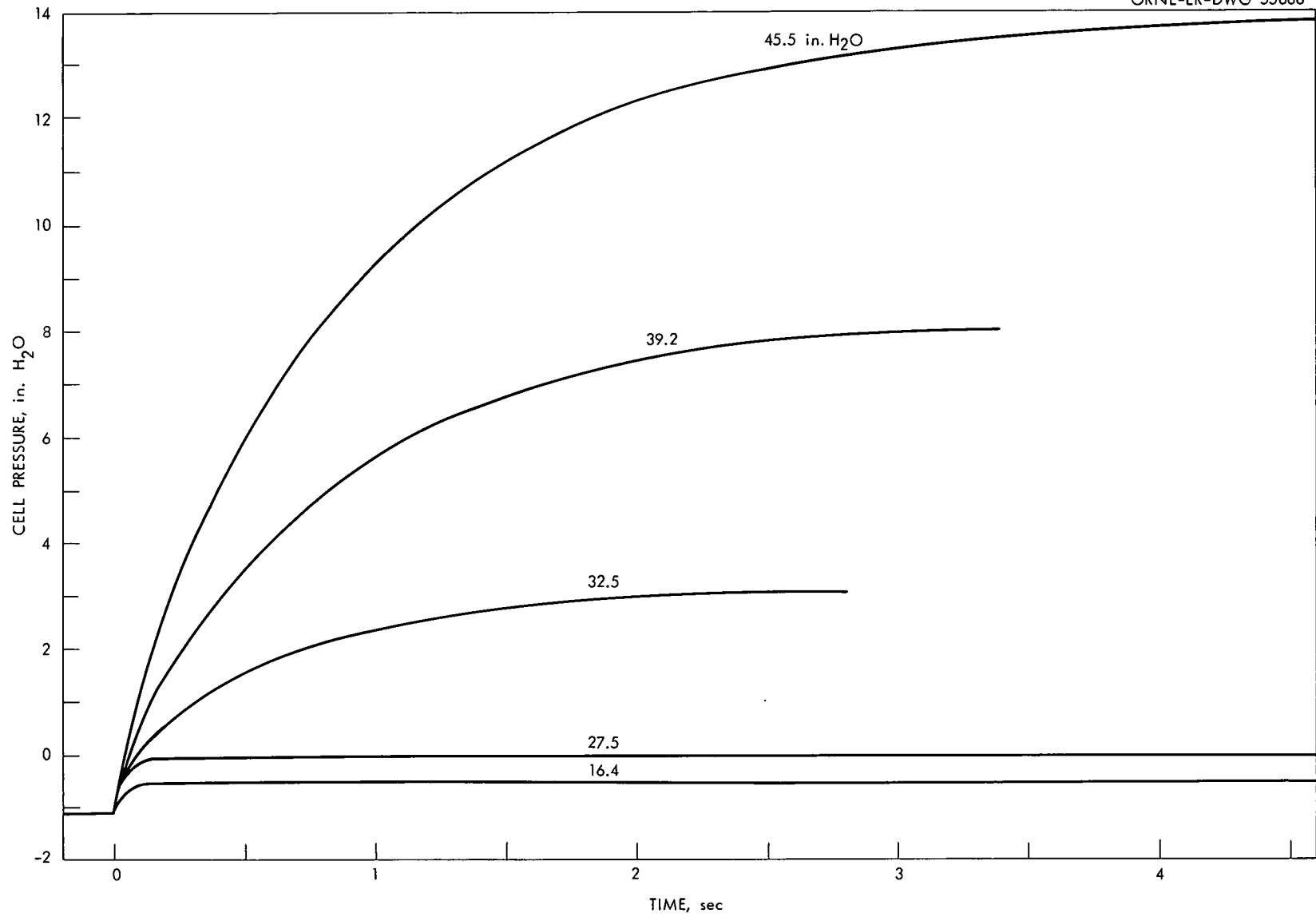


Fig. 34. Effects of ramp perturbations on cell pressure Bldg. 4507.

ORNL-3086
UC-38 - Engineering and Equipment
TID-4500 (16th ed.)

INTERNAL DISTRIBUTION

- | | |
|-------------------------------------|---------------------------------|
| 1. Biology Library | 47. M. T. Kelley |
| 2-3. Central Research Library | 48. J. A. Lane |
| 4. Reactor Division Library | 49. T. A. Lincoln |
| 5. ORNL - Y-12 Technical Library | 50. S. C. Lind |
| Document Reference Section | 51. K. Z. Morgan |
| 6-25. Laboratory Records Department | 52. J. P. Murray (K-25) |
| 26. Laboratory Records, ORNL R.C. | 53-55. J. J. Perona |
| 27. E. D. Arnold | 56. D. Phillips |
| 28. R. E. Blanco | 57. H. E. Seagren |
| 29. G. E. Boyd | 58. M. J. Skinner |
| 30. J. C. Bresee | 59. J. A. Swartout |
| 31. K. B. Brown | 60. E. H. Taylor |
| 32. F. R. Bruce | 61. J. W. Ullmann |
| 33. C. E. Center | 62. W. E. Unger |
| 34-35. F. L. Culler | 63. A. M. Weinberg |
| 36. D. E. Ferguson | 64. M. E. Whatley |
| 37. J. H. Frye, Jr. | 65. C. E. Winters |
| 38. J. H. Gillette | 66. R. G. Wymer |
| 39. H. E. Goeller | 67. J. W. Youngblood |
| 40. A. T. Gresky | 68. D. L. Katz (consultant) |
| 41. W. R. Grimes | 69. C. E. Larson (consultant) |
| 42. C. E. Guthrie | 70. I. Perlman (consultant) |
| 43. A. Hollaender | 71. J. H. Rushton (consultant) |
| 44. A. S. Householder | 72. H. Worthington (consultant) |
| 45. R. G. Jordan (Y-12) | 73. T. H. Pigford (consultant) |
| 46. W. H. Jordan | |

EXTERNAL DISTRIBUTION

74. Division of Research and Development, AEC, ORO
75-549. Given distribution as shown in TID-4500 (16th ed.) under Engineering and Equipment category (75 copies - OTS)